NGU
Norges geologiske undersøkelse
Geological Survey of Norway

Geological Survey of Norway
NO-7441 Trondheim, Norway
Tel.: 47 73 90 40 00
Telefax 47 73 92 16 20

REPORT

Report no.: 2005.044 | ISSN 0800-3416 | Grading: Open

Title:
Interpretation of the magnetic anomaly pattern in the Oslo region

Authors:
Lundin, E., Olesen, O., Kihle, O., J.R. Skilbrei

Client:

County:

Commune:

Map-sheet name (M=1:500.000)
Skien, Oslo, Hamar

Map-sheet no. and -name (M=1:50.000)
1815 I Gran – 1915 IV Hurdal
1815 II Oppkuven - 1915 III Nannestad
1814 I Asker – 1914 1V Oslo
1814 II Drøbak - 1914 III Ski
1813 I Horten – 1913 IV Vannsjø
1813 II Tjøme – 1913 III Fredrikstad

Deposit name and grid-reference:

Number of pages: 43 Price (NOK): 400,-
Map enclosures: 1

Fieldwork carried out:	Date of report:	Project no.:	Person responsible:
2004	10.06.2005	301809	Jan S. Rønning

Summary:
The Permian Oslo Field contains a large number of interesting magnetic anomalies associated with magmatic rock bodies (lavas, dikes, calderas, and plutons). The area is characterized by large-scale circular to elliptical anomalies related to calderas and plutons, and by linear magnetic anomalies of various trends. The linear anomalies can be subdivided into three genetically different groups, which relate to: 1) Precambrian basement foliation and Paleozoic bedding, 2) Permian dikes that in turn often follow faults, 3) deep weathering of pre-existing weaknesses (joints, faults, and possibly dikes). The first group is not of particular interest to this study and is readily excluded by comparing the anomalies with the geologic map. Anomalies related to dikes and deep weathering tend to crosscut the geology and are hence also easy to distinguish. Separating dikes from deeply weathered joints and faults can be more difficult. By in large, deeply weathered joints tend to have a negative anomaly and correlate with linear topographic depressions. Generally, dikes tend to have a positive anomaly, although dikes with negative anomalies do exist. Field checks of the anomalies can generally test if a trend in an area relates to dikes or weathering. A criteria that also helps separating weathering from dikes is the width of the anomalies – those associated with deep weathering tend to be wider than the dike anomalies.

Dikes are often more fractured than the host rock and therefore, tend to be groundwater bearing. Deeply weathered joints and fractures, on the other hand, are filled with tight clays and have low permeability. Such clay-bearing joints and fractures are commonly unstable during tunnelling.

A previously unreported large (ca. 22 to 24 km) elliptic negative anomaly is recognized around the Drammen caldera. It is unclear what the source of the anomaly is but it is tentatively suggested to relate to the outer limit of the Drammen granitic pluton. The very centre of the Drammen caldera is marked by a pronounced negative anomaly, of –1000 to –1500 nT. This anomaly may relate to basalts located centrally in the caldera, or alternatively to a late stage central intrusion. However, no such intrusive rocks have been mapped to date, and if this is the case the intrusive rocks must be located beneath the exposed lava or be unrecognised.

Keywords: Geophysics (geofysikk)	Bedock geology (Bergrunnsgeologi)	Magnetic anomaly (magnetisk måling)
Caldera (kaldera)	Deep weathering (dypforvittring)	Dike (gang)
Topography (topografi)		Scientific report (Fagrapport)

CONTENTS

FIGURES

15	Combination of aeromagnetic data and topographic data.
16a	Pre-Cretaceous regolith (etch) surface in the Hvaler area.
16b	Pre-Cretaceous regolith (etch) surface in the Sarpsborg area.
16c	Pre-Cretaceous regolith (etch) surface in the Fredrikstad area.
17	Schematic illustration of the process leading to the present day deep weathering products.
18a	Magnetic modelling of a profile
18b	Location map for modelled profile.
19a	Magnetic anomaly map over Fredrikstad area
19b	Profile 7 – Vesterøy-Spjærøy-Asmaløy area (south of Fredrikstad)
19c	Profile 8 - 18c. Profile 8 - north of Fredrikstad.
20a	Magnetic anomaly map of Hurum area.
20b	Profile 11 – Hurum area.
21a	Magnetic anomaly map of Drammen area.
21b	Profile 18 showing a general relationship between magnetic anomalies (red) and topography (green).
22a	Magnetic anomaly map of Lier to Asker area with the Lieråsen railroad tunnel shown in black/white.
22b	Interpreted map of Lier to Asker area with the Lieråsen railroad tunnel
23a	Magnetic anomaly map of Drammen caldera area
23b	Geologic map of Drammen area draped over the magnetic field.
23c	Profile 21-24 in Drammen caldera area.
24	Generalized evolution of caldera.
25	Shaded topographic image of the Valles caldera, New Mexico.
26	Structure maps of a) the Silverton/Lake City calderas in the San Juan Mountains, Colorado and b) the Maroa/Okataina/Rotorua calderas in north Iceland.

APPENDIX

1: 500,000 maps.

Map 7	Interpreted magnetic anomalies in the Oslo area overlain on the Oslo Field geologic map.

In addition the following 1:50,000 magnetic anomaly maps, covering two 1:50,000 sheets each, are processed and are available from NGU on request:

From north to south:

Map 1	1815 I Gran – 1915 IV Hurdal
Map 2	1815 II Oppkuven - 1915 III Nannestad
Map 3	1814 I Asker – 1914 1V Oslo
Map 4	1814 II Drøbak - 1914 III Ski
Map 5	1813 I Horten – 1913 IV Vannsjø
Map 6	1813 II Tjøme – 1913 III Fredrikstad

1. INTRODUCTION

This work has been carried out as a part of the GEOS project in the greater Oslo region. The main objective of the work has been to separate the sources of linear magnetic anomalies, in particular separating dikes from deeply weathered fractures and faults. The implication of separating these features is that dikes tend to enhance bedrock permeability and hence be preferable sites for drilling for groundwater while deeply weathered fractures and faults tend to have the opposite effect. The reason for the reduced permeability of deeply weathered joints and faults is the presence of fine-grained clay products. Understanding this difference is particularly important for tunnel projects since the clays in deeply weathered faults and fractures often are unstable.

The magnetic data used in the project have been merged from the following NGU aeromagnetic surveys: Gran, Hurdal, Oppkuven, Fugro, Skien, Siljan, Torp, Larvik1, Larvik2, Larvik10. The topographic data used was a digital elevation model with 30 m resolution.

The magnetic anomalies were interpreted with ARC Map, which is a GIS program. Profiles were extracted from the magnetic and topographic data with Geosoft.

Some images show the 1:250,000 scale Geologic map of the Oslo Field draped over a black and white version of the total magnetic field. These were derived from the ArcMap project.

Locations of more detailed maps are shown on the index map. The square mesh on the detailed figures represent 1x1 km cells.

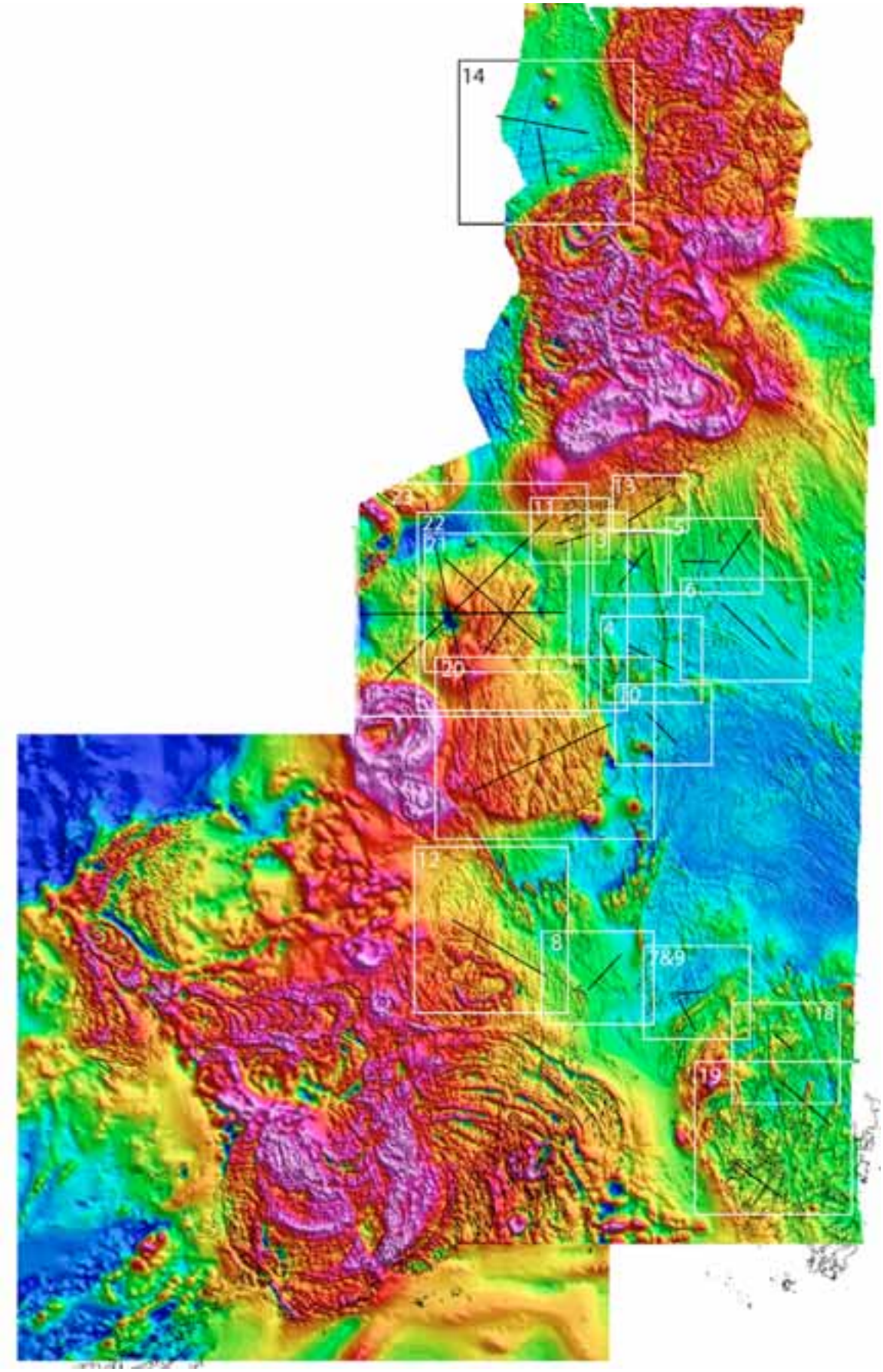

Fig. 1. Index map of merged magnetic data in GEOS area. Numbered white boxes refer to figures of more detailed maps. Black lines with the boxes relate to profiles.

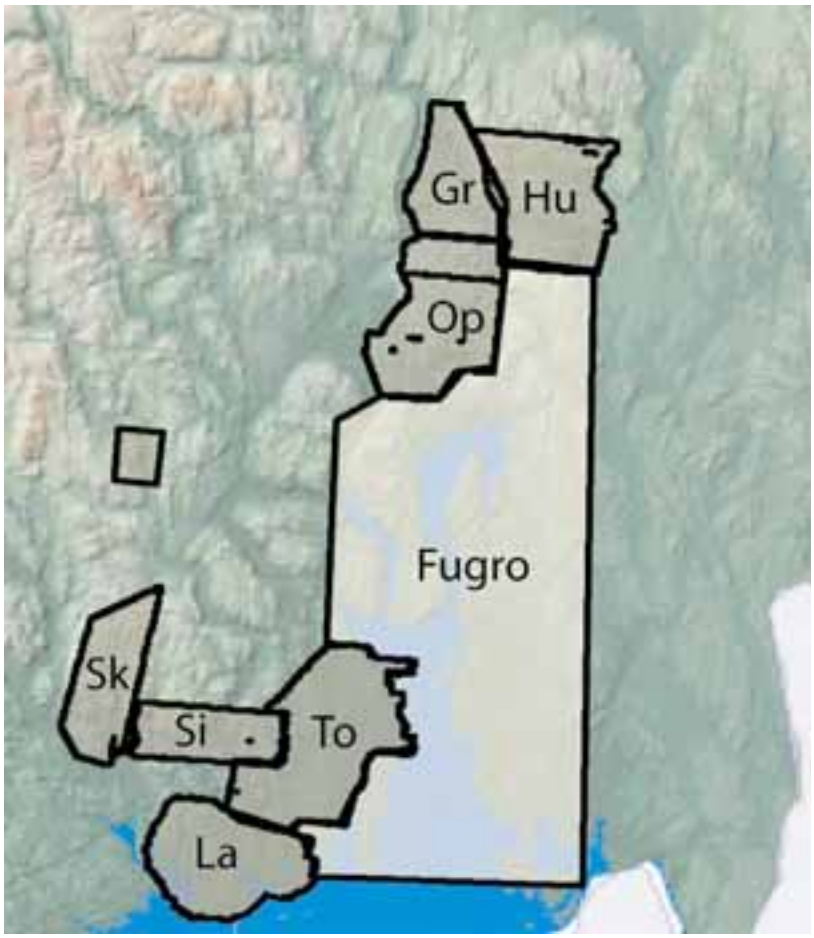

Fig. 2a. Aeromagnetic database. Abbreviations for individual aeromagnetic surveys: Gr = Gran, Hu = Hurdal, Op = Oppkuven, La = Larvik1, Larvik2, and Larvik 10, Si = Siljan, Sk = Skien and To = Torp.

The following references describe the acquisition and processing of the airborne data from the above areas:

Gran and Oppkuven = Beard, 1998; Beard & Rønning, 1997
Fugro = Fugro, 2003
Hurdal = Beard & Mogaard, 2001
Larvik = Beard, 1999; Mogaard, 1998
Siljan = Håbrekke, 1982
Skien = Mogaard & Beard, 2000
Torp = Mogaard, 2001

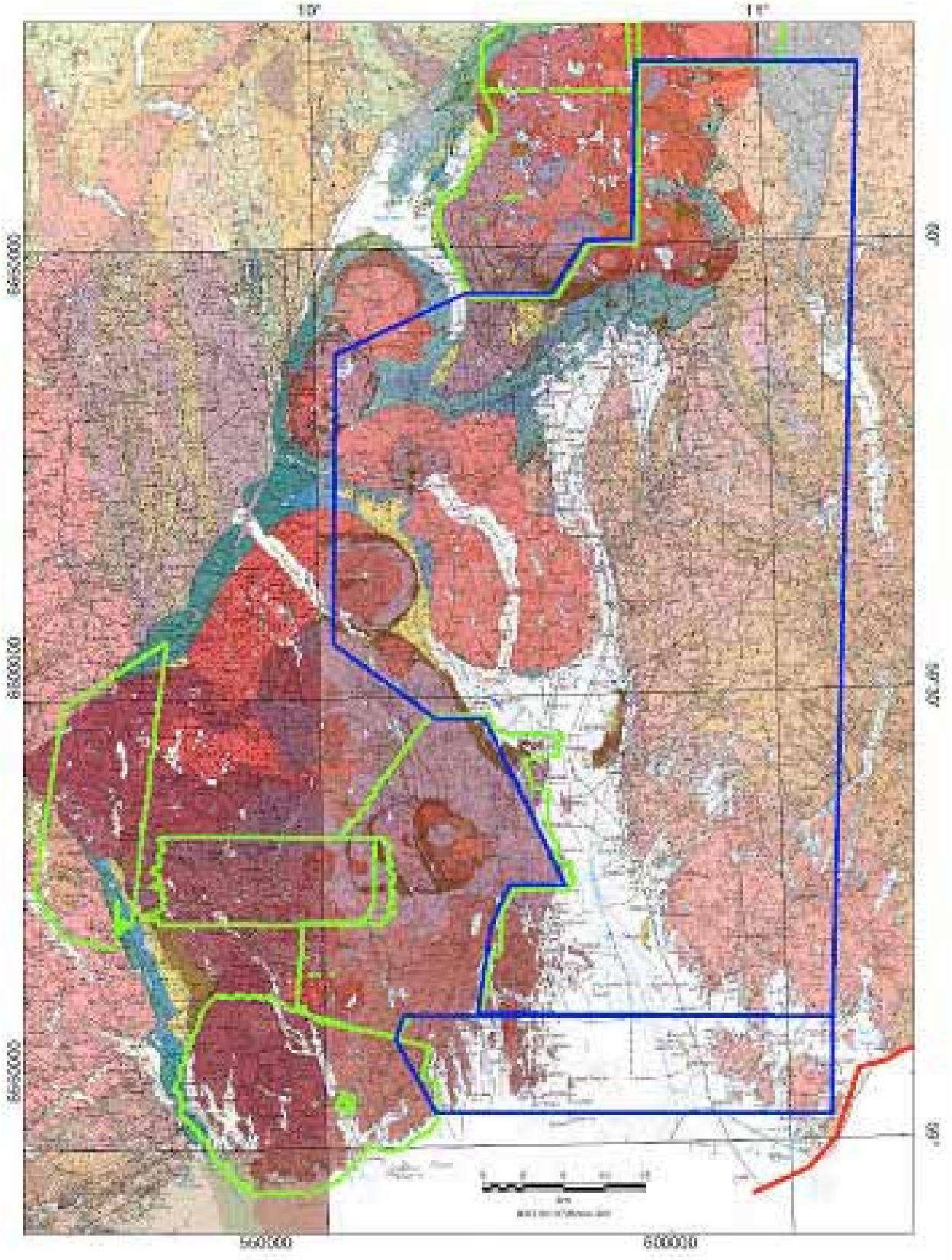

Fig. 2b. Aeromagnetic database in relationship to the geologic map of the area.

2. LINEAR MAGNETIC ANOMALIES IN THE GEOS AREA

2.1 Linear anomalies interpreted to be associated with dikes

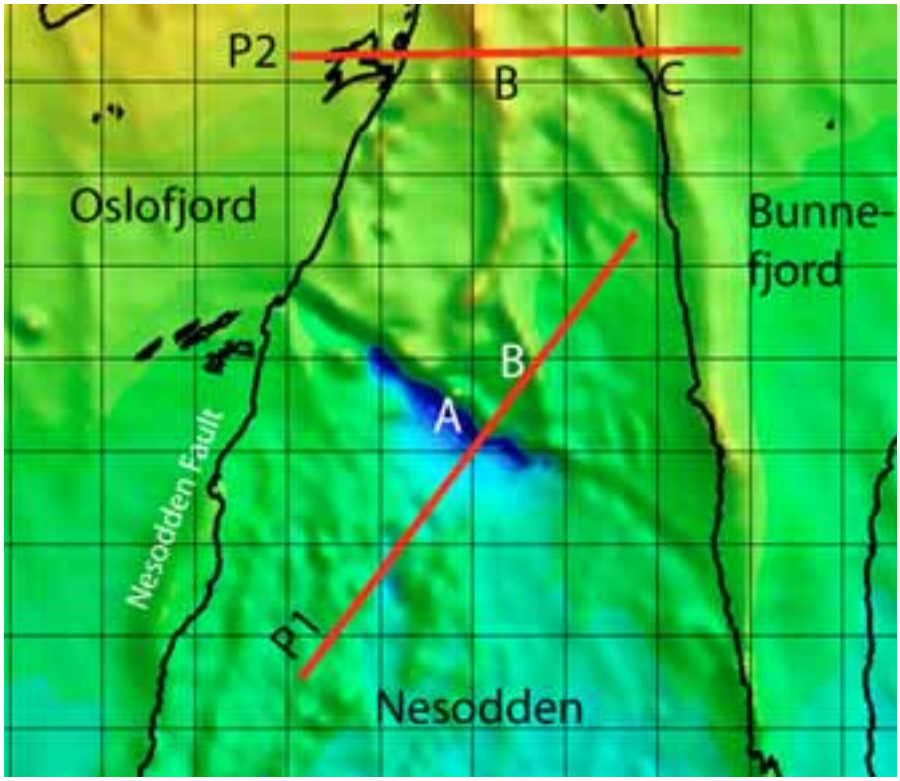

Fig. 3a. Magnetic anomaly map of northern Nesodden, with high-pass filtered data set for shaded relief. Anomaly A is crosscuts the bedrock of the area and appears related to a set of diabase dikes (Figs. 3b and 3c).

Fig. 3b. Outcrop of the NW-trending dike set along the western shore of Nesodden, just north of Alvern. Photo B.T. Larsen.

Fig. 3c. Outcrop of NW-trending diabase dike set along road just east of Alvern, associated with anomaly A in Fig. 3a. UTM coordinates of photo location: 591,200 - 6632,680.

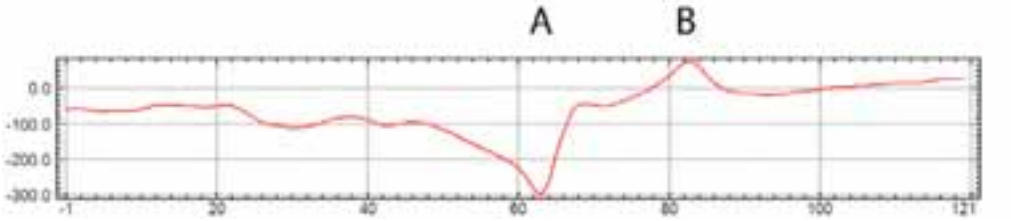

Fig. 3d. Profile 1. NW-trending symmetric negative magnetic anomaly A, associated with the dike set that intersects the Nesodden fault just north of Alvern. Several dikes, associated with the anomaly, are well exposed on the western shore (Fig. 3b) and further inland along road cuts (Figs. 3c) Anomaly B is interpreted to mark a dike, and is also seen in Profile 2.

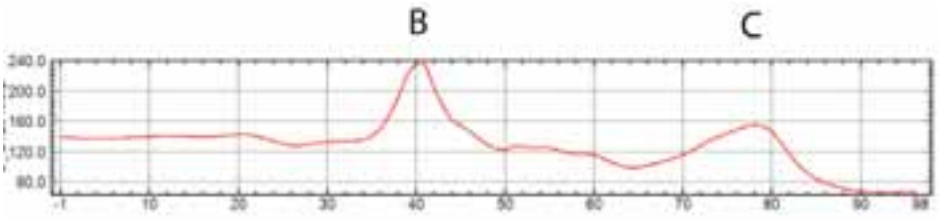

Fig. 3e. Profile 2. North-trending positive magnetic anomalies. Anomaly B is interpreted to represents a dike (and fault?). Anomaly C, which follows the eastern shoreline to Nesodden, is an intruded fault (dike-intruded fault) and appears to be continuous with anomaly E on Profile 3 (Fig. 4b). Anomaly E represents a syenite dike, sampled at Neset by O. Olesen, 2004.

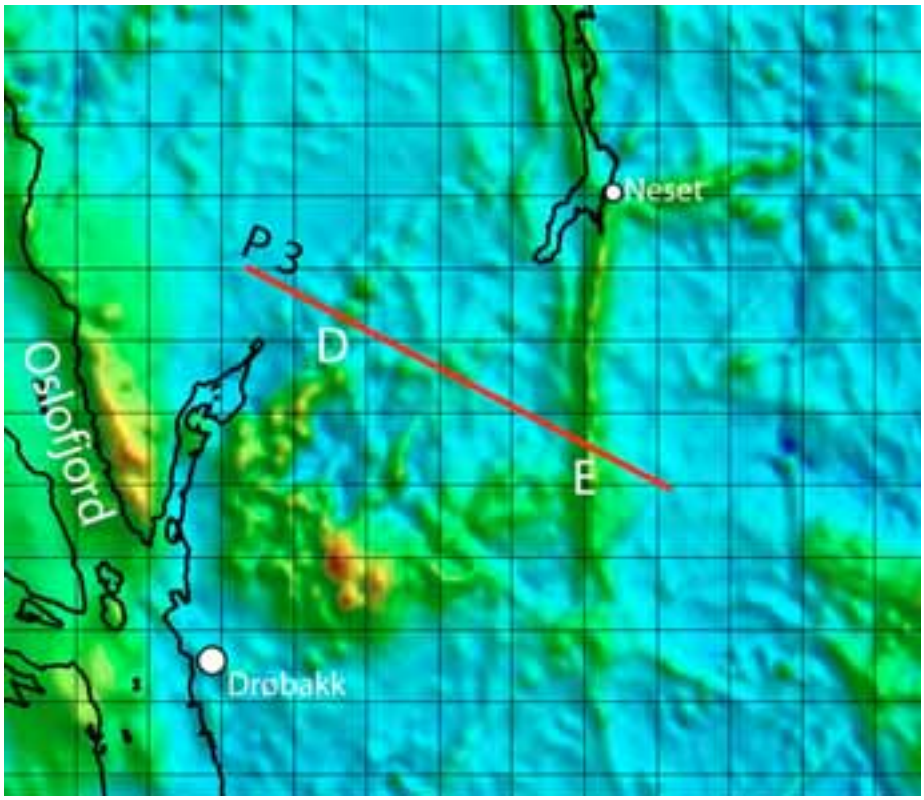

Fig. 4a. Magnetic anomaly map over Drøbak area.

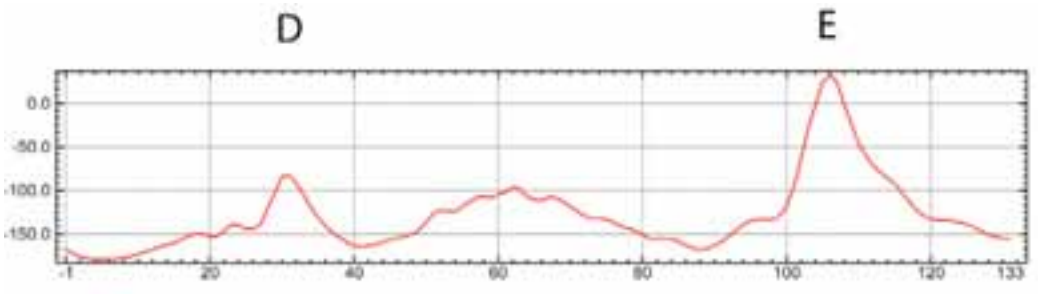

Fig. 4b. Profile 3. The NE-trending positive anomaly D is interpreted as a dike, while anomaly E is interpreted as the southern continuation of anomaly C (Figs. 3a and 3d), i.e. a combined normal fault and dike. Anomaly E is a syenite dike, sampled at Neset by O. Olesen, 2004.

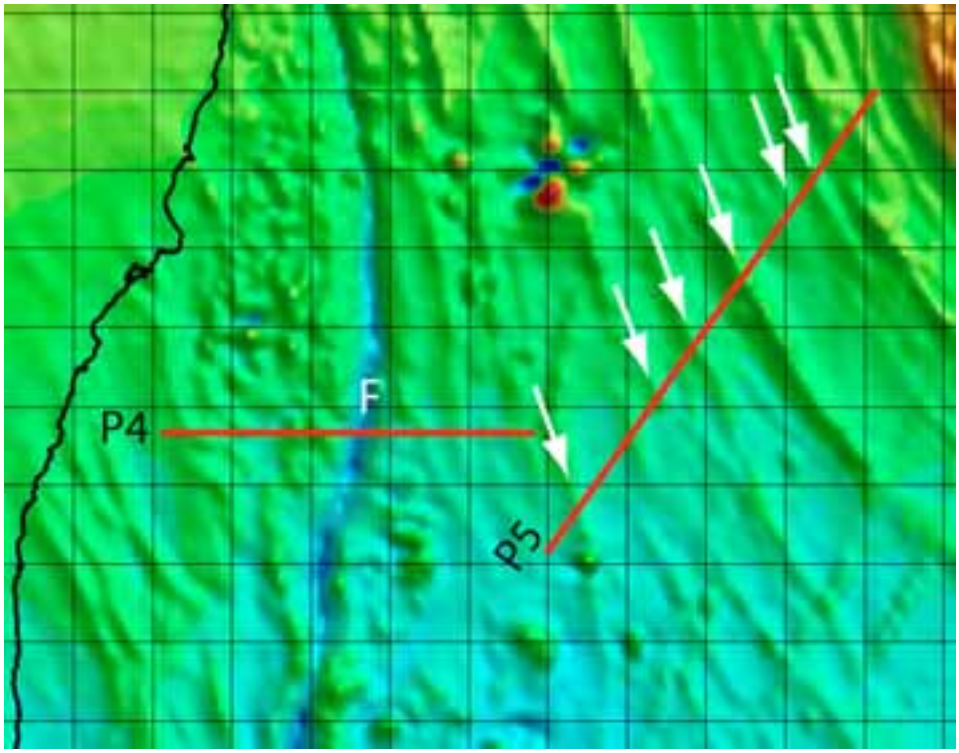

Fig. 5a. Magnetic anomaly map of southern Oslo area showing a prominent N-trending negative anomaly F related to a rhomb-porphyry dike. Numerous NW-trending positive anomalies (white arrows) are caused by lithologic boundaries within folded Pre-Cambrian fold basement.

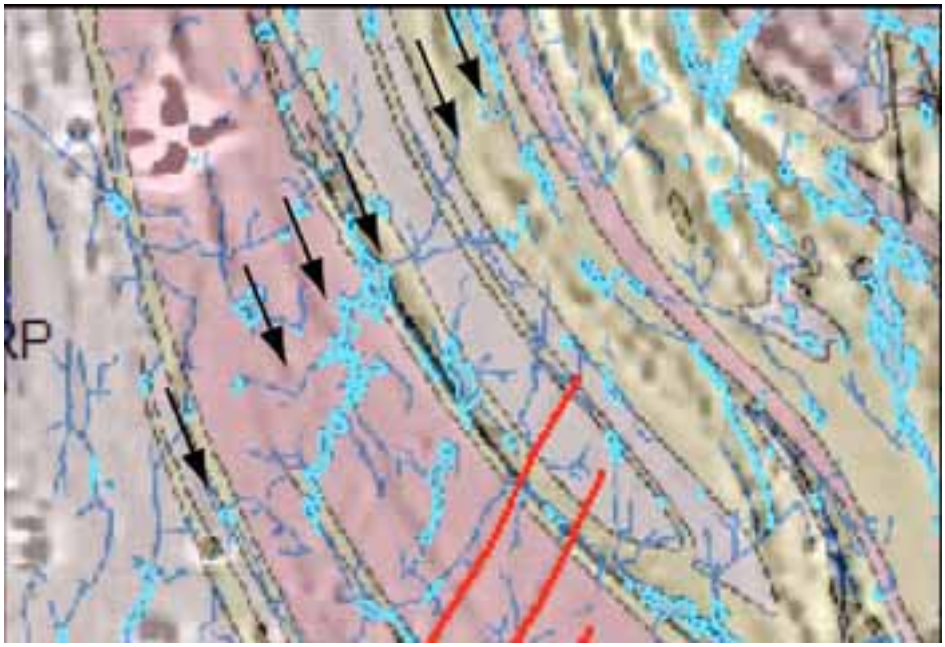

Fig. 5b. Geologic map of the Oslo field draped over magnetic anomaly map (Fig. 5a). The arrows are located in the same place as on the magnetic anomaly map. The coincidence between the anomalies and bedrock boundaries suggest lithologic control from basement boundaries.

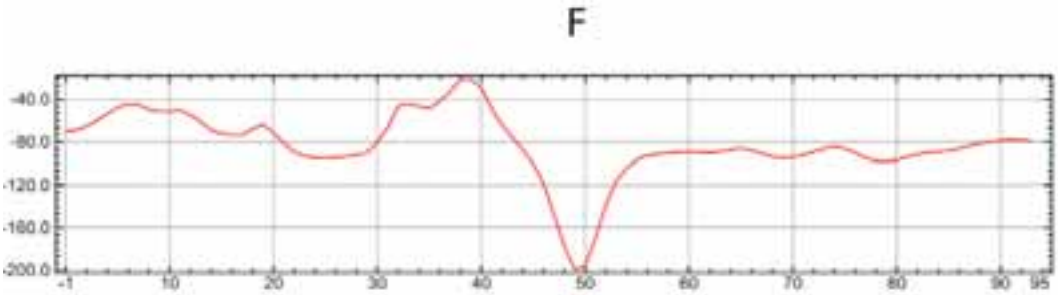

Fig. 5c. Profile 4. The marked negative anomaly F is part of a c. 30 km long continuous anomaly representing a rhomb-porphyry dike.

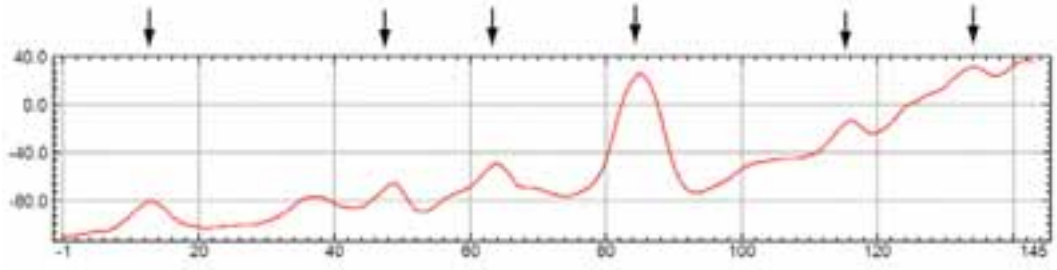

Fig. 5d. Profile 5 across southern Oslo area revealing positive anomalies related to lithologic boundaries (compare Fig. 5b).

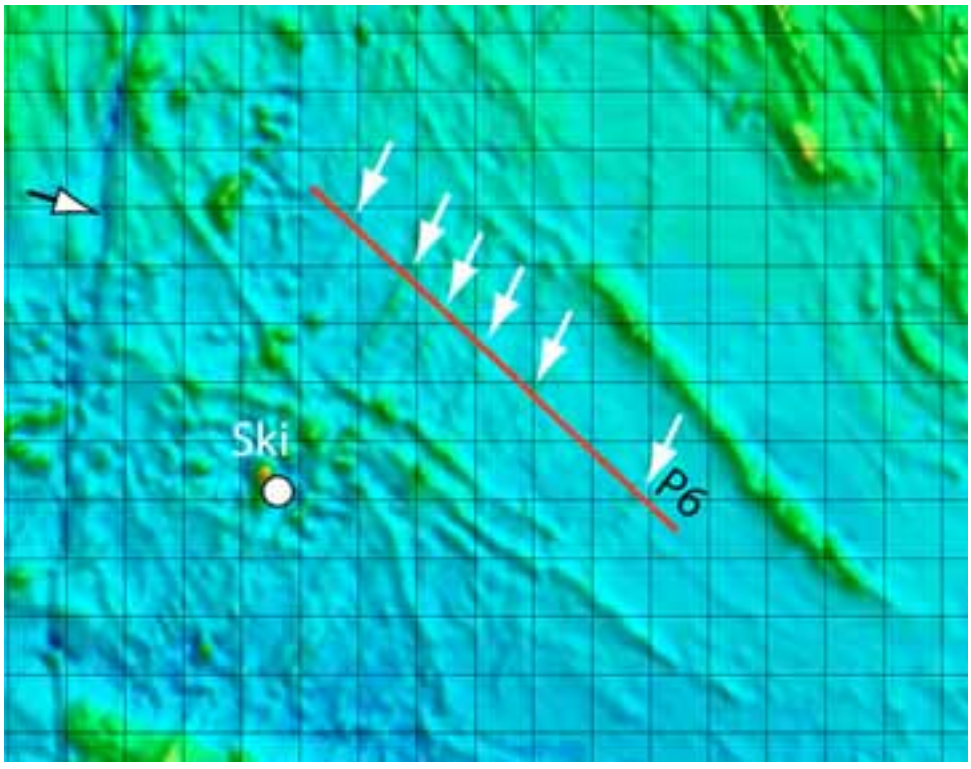

Fig. 6a. Magnetic anomaly map of Ski area, displaying a series of positive anomalies, interpreted to relate to NE-trending dike swarm. Arrows point to discrete anomaly peaks (see profile below). The easternmost arrow points to an anomaly that is proven to relate to a diabase dike (Fig. 6b). The NW-trending positive anomalies relate to lithologic boundaries in the Precambrian basement (same as in Fig. 5b). The black and white arrow points to a N-trending negative anomaly, which is the same rhomb-porphyry dike as in Fig. 5a (Anomaly F).

Fig. 6b. Photo of topographic depression associated with an outcropping diabase dike in the Ski area (easternmost anomaly in Fig. 6a). UTM coordinates of photo location 608,860 – 6619,650.

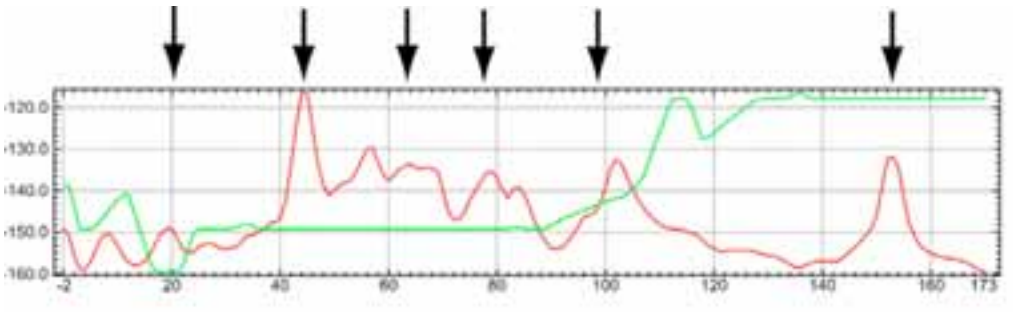

Fig. 6c. Profile 6. Positive magnetic anomalies (red) interpreted to represent NE-trending dikes. The easternmost anomaly is a sampled diabase dike (Fig. 6b). Note the lack of association with topography (green), in contrast to the areas interpreted to be characterized by deep weathering.

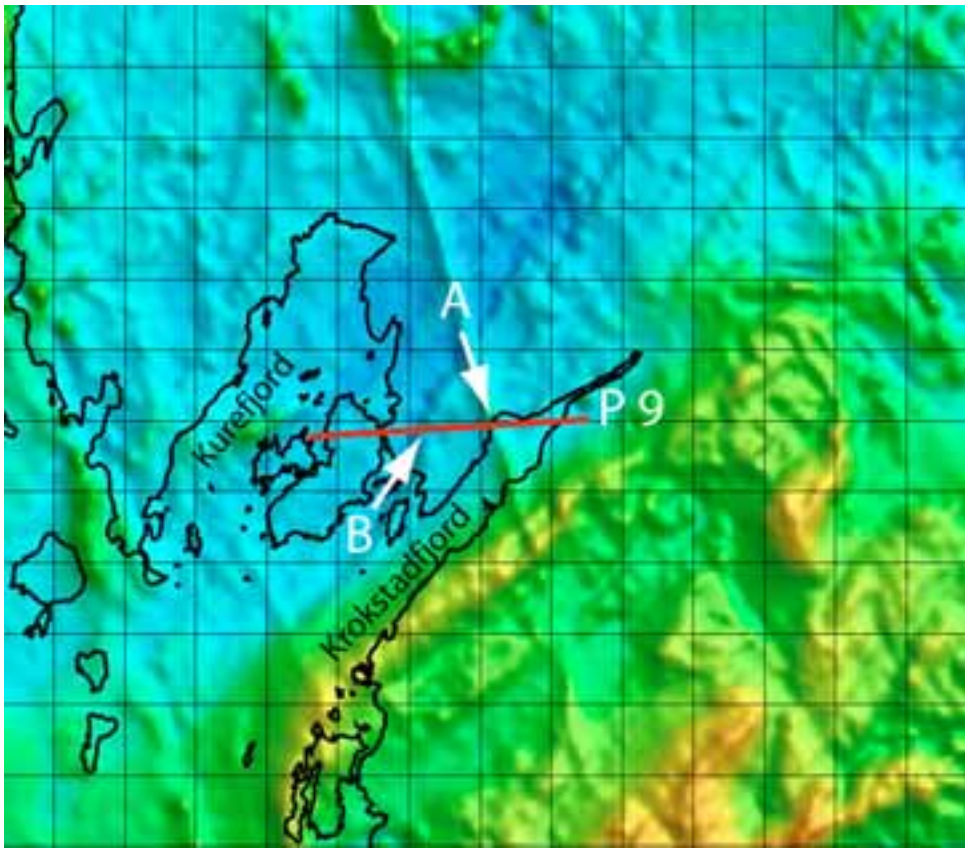

Fig. 7a. Magnetic anomaly map of Krokstadfjord area, showing two crossing anomaly trends. The NNW-trending positive anomaly (A) is an established dike. The NE-trending positive anomalies (B) are interpreted as dikes.

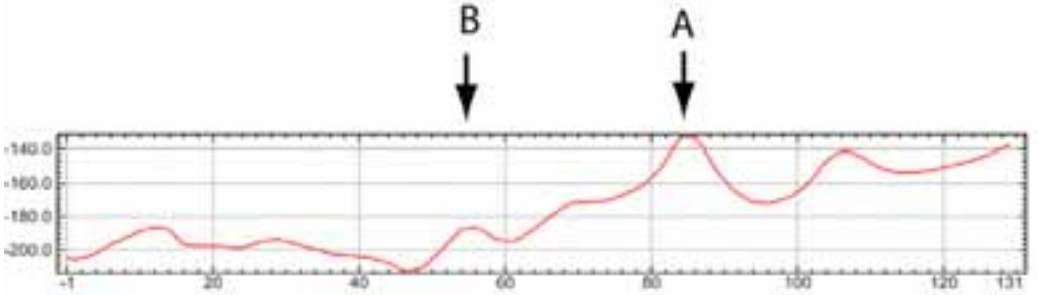

Fig. 7b. Profile 9. Magnetic anomaly A relates to a diabase dike, outcropping at UTM 600850 –6678100 on map sheet 1913 III. Anomaly B is interpreted to represent one of many NE-trending dikes.

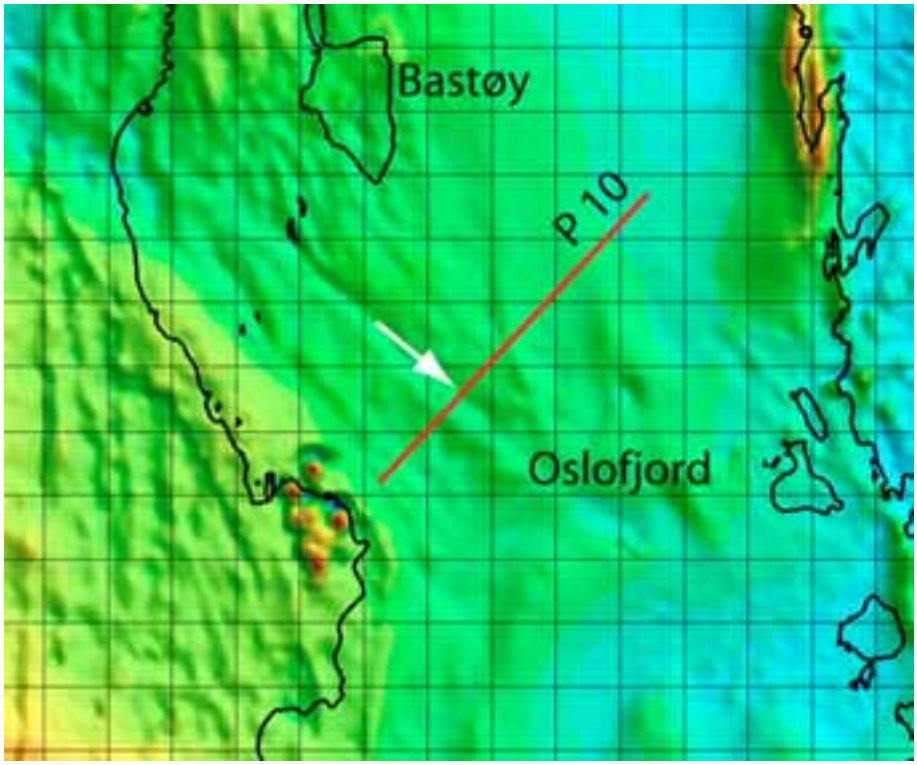

Fig. 8a. Magnetic anomaly map of area south of Horten illustrating a NW-trending negative anomaly, interpreted to represent a fault (intruded by a dike?).

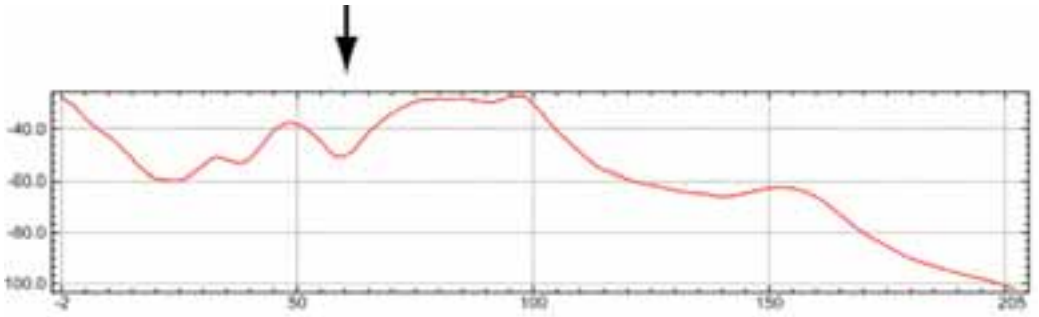

Fig. 8b. Profile 10. Arrow points to the NW-trending negative anomaly seen on map above, and is interpreted to represent a fault (possibly intruded by a dike).

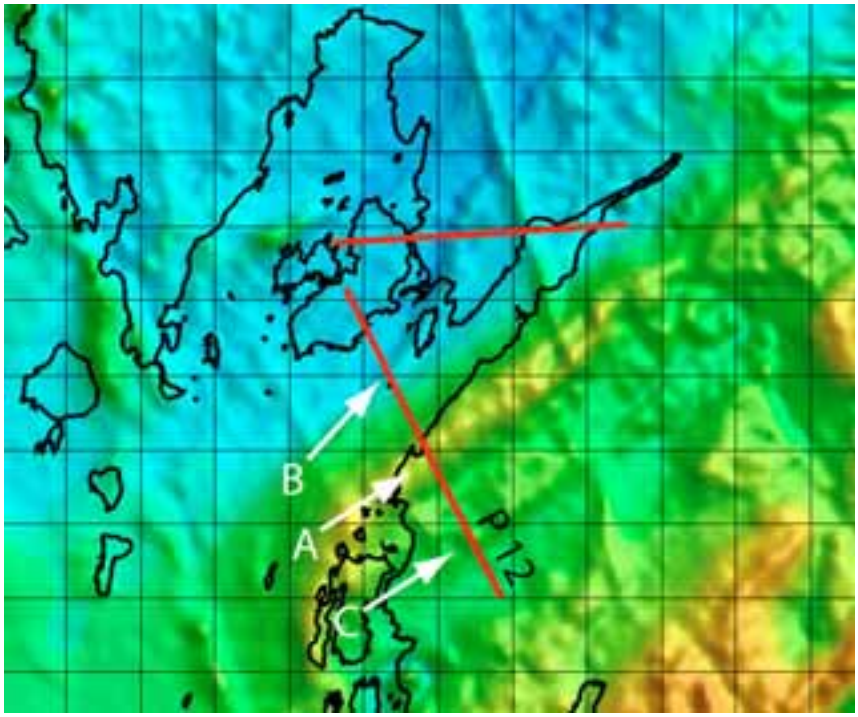

Fig. 9a. Magnetic anomaly map of Krokstadfjord area (compare Fig. 7a)

Fig. 9b Geologic map of the Oslo field draped over magnetic anomalies. Same arrows and labels as above. Anomaly A lies close to the contact between the granite to the south and the gneiss to the north and is therefore likely related to the change in lithology.

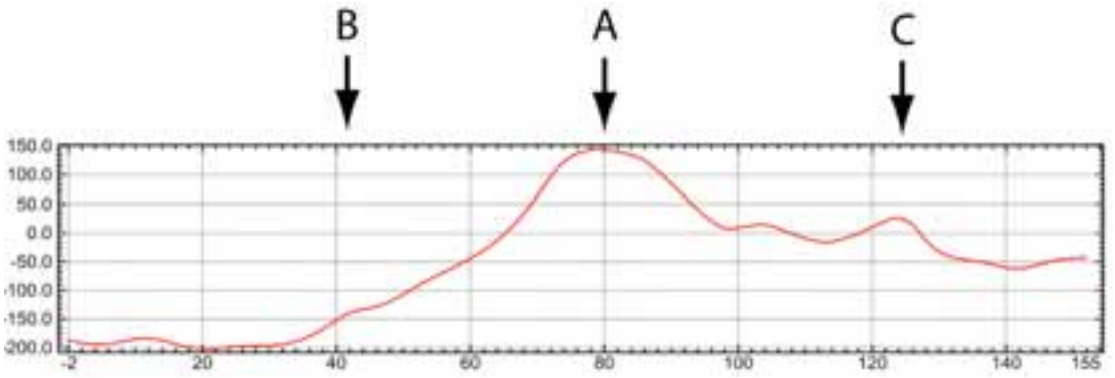

Fig. 9c. Profile 12. Anomaly A is likely caused by lithology. It is located at the boundary between granite to the south (right) and tonalitic gneiss to the north. Anomaly B is the southern continuation of anomaly B in Fig. 7a and is interpreted to be a dike. Anomaly C is uncertain but could be a dike.

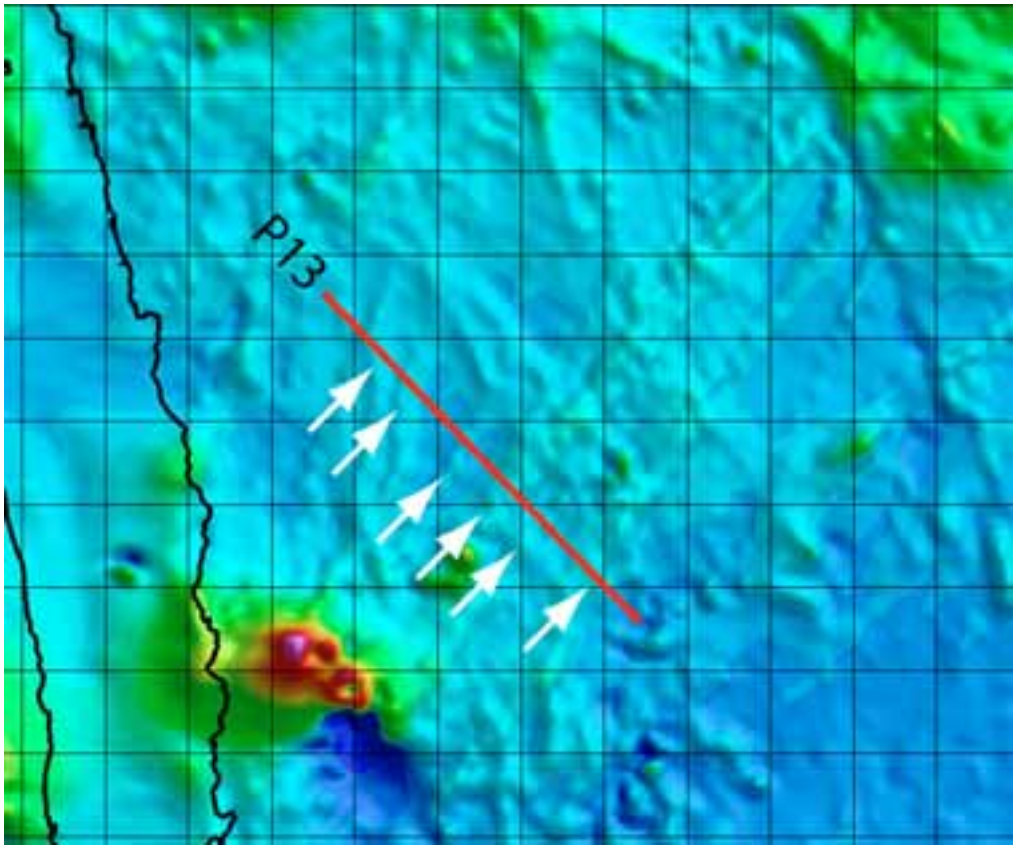

Fig. 10a. Magnetic anomaly map of the Hvitsten area. The distinct positive anomaly SW of the profile is an essexite intrusion. The arrows point toward an interpreted NE-trending dike swarm. These are the same anomalies/dikes as those shown in the Ski area (Fig. 6a)

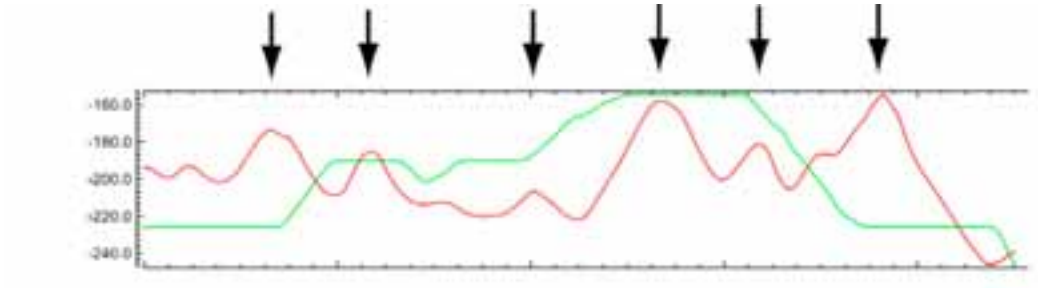

Fig. 10b. Profile P 13. The arrows point toward the positive anomalies interpreted as dikes. Green line represents bathymetry.

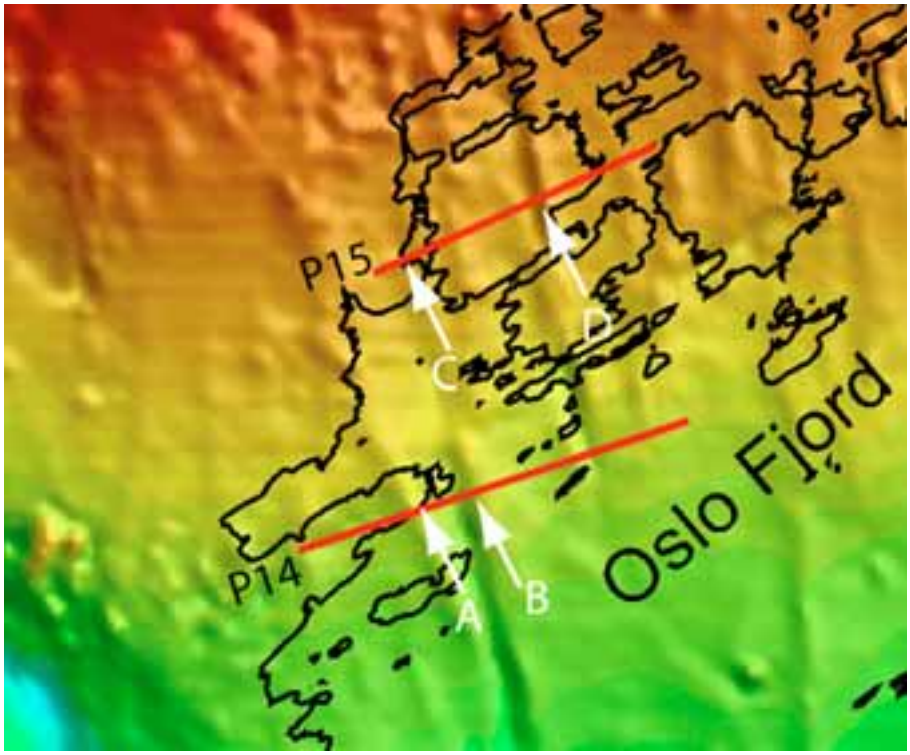

Fig. 11a. Magnetic anomaly map of the inner Oslo Fjord, NW of Nesodden.

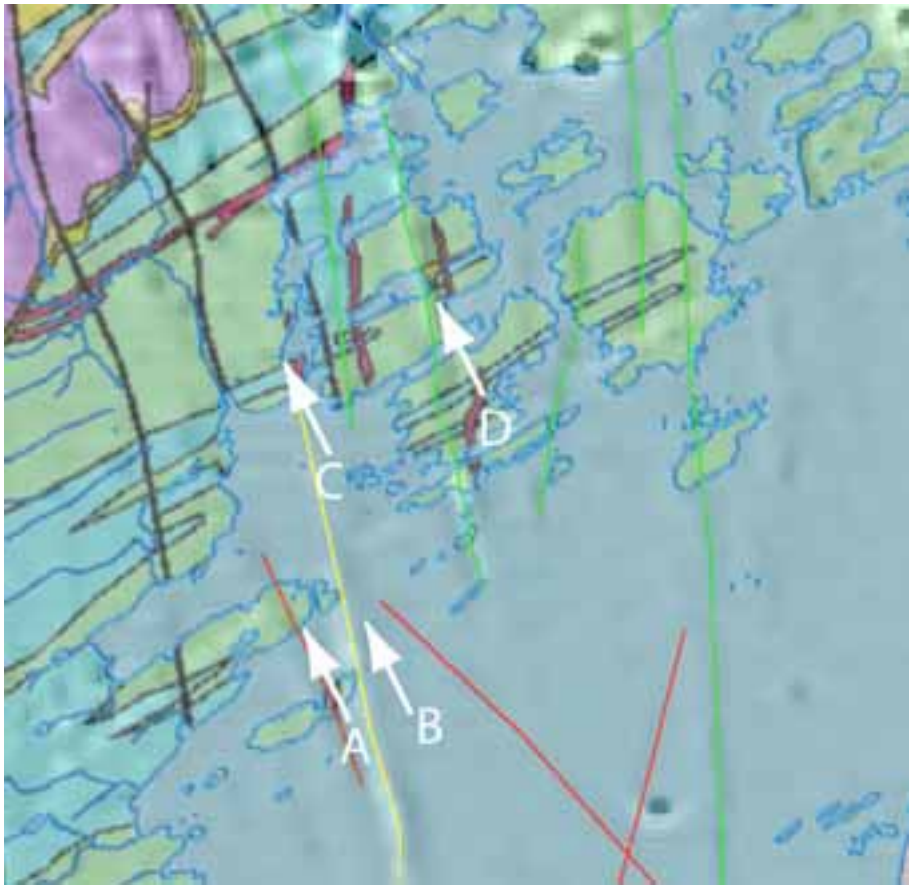

Fig. 11b. Geologic map draped over magnetic anomalies. Anomaly B is the possible offshore continuation of a mapped fault, and anomaly D is close to a mapped dike.

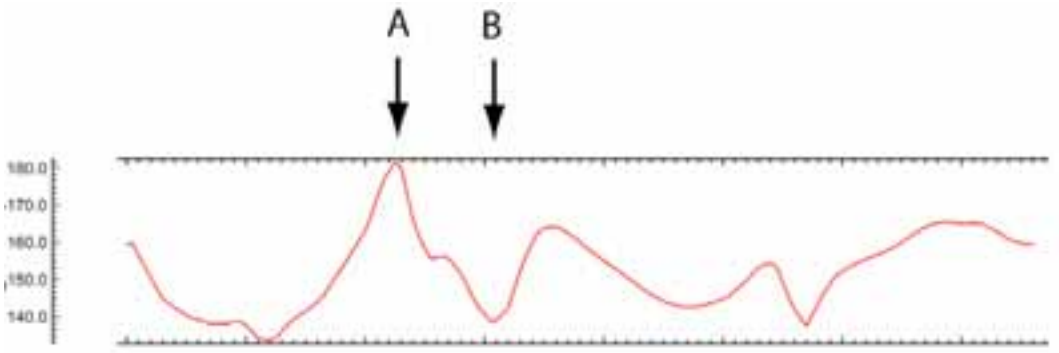

Fig. 11c. Profile 14. Positive anomaly A is interpreted as a dike. Negative anomaly B is interpreted as a fault, possibly intruded by a dike.

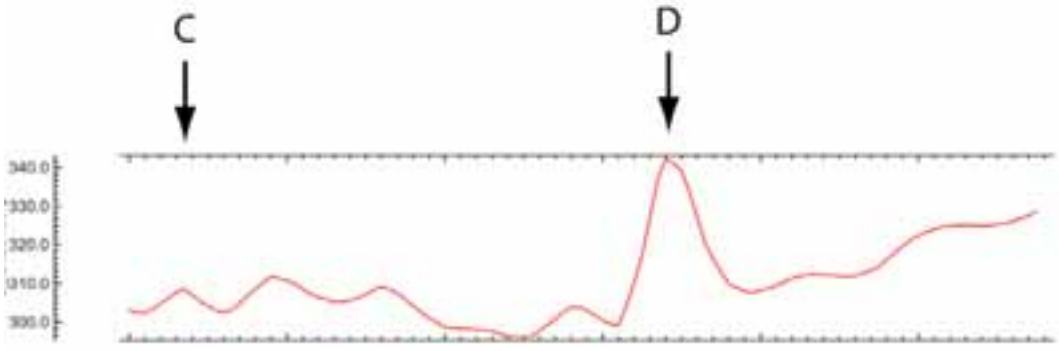

Fig. 11d. Profile 15. Anomaly C is the northern continuation of anomaly B on profile 14, i.e. the likely northerly continuation of a positive dike. Positive anomaly D is a mapped dike.

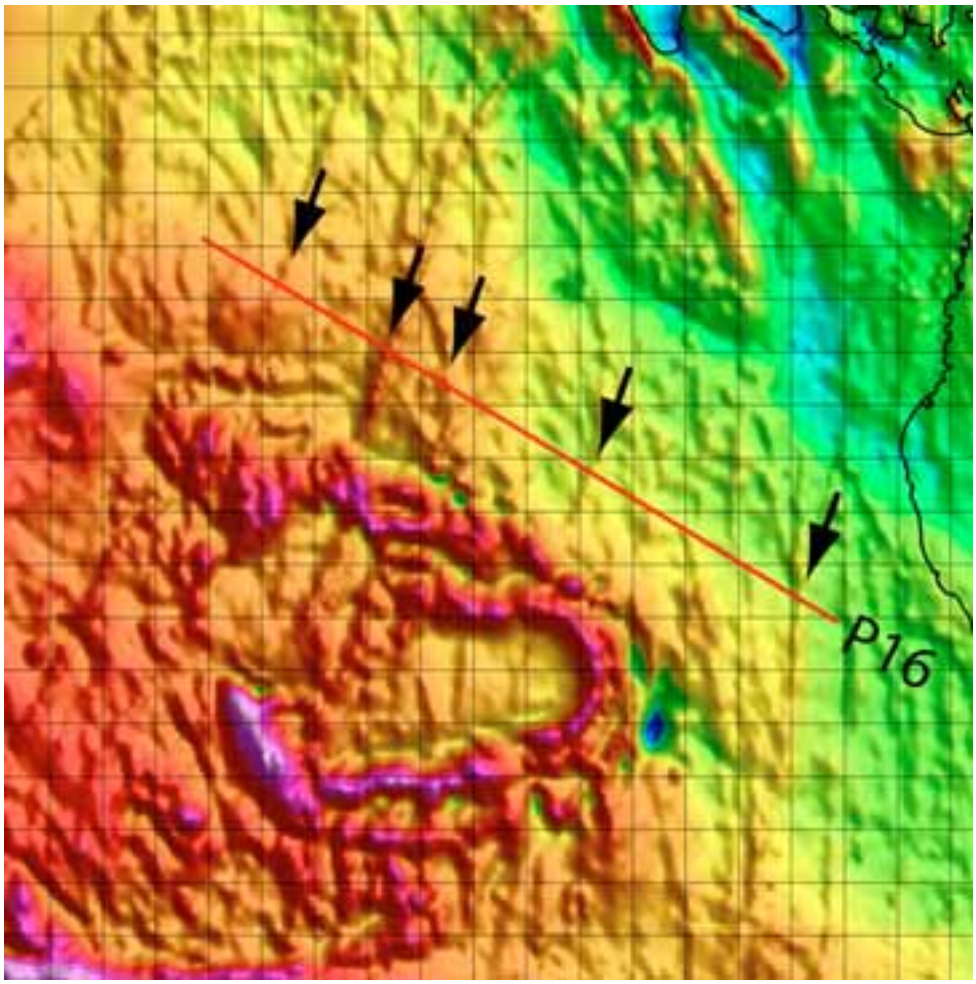

Fig. 12a. Magnetic anomaly map of the Ramnes area. The pronounced elliptical positive anomaly is the ring fracture zone of the Ramnes caldera. The NE-trending positive anomalies are interpreted as dikes, postdating the caldera collapse. The second arrow from the left probably represents an intruded fault since the anomaly generates an offset of the coastline to the north.

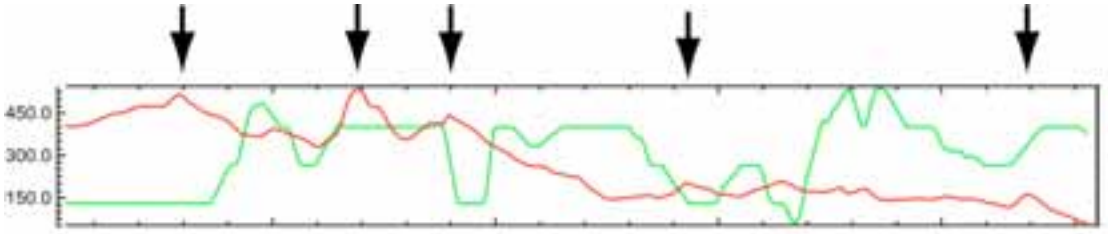

Fig. 12b. Profile 16. Positive magnetic anomalies (black arrows) are interpreted to represent dikes. These dikes must postdate the caldera collapse phase since they extend through the circular anomalies. There is no correlation between the linear magnetic anomalies (red) and the topography (green).

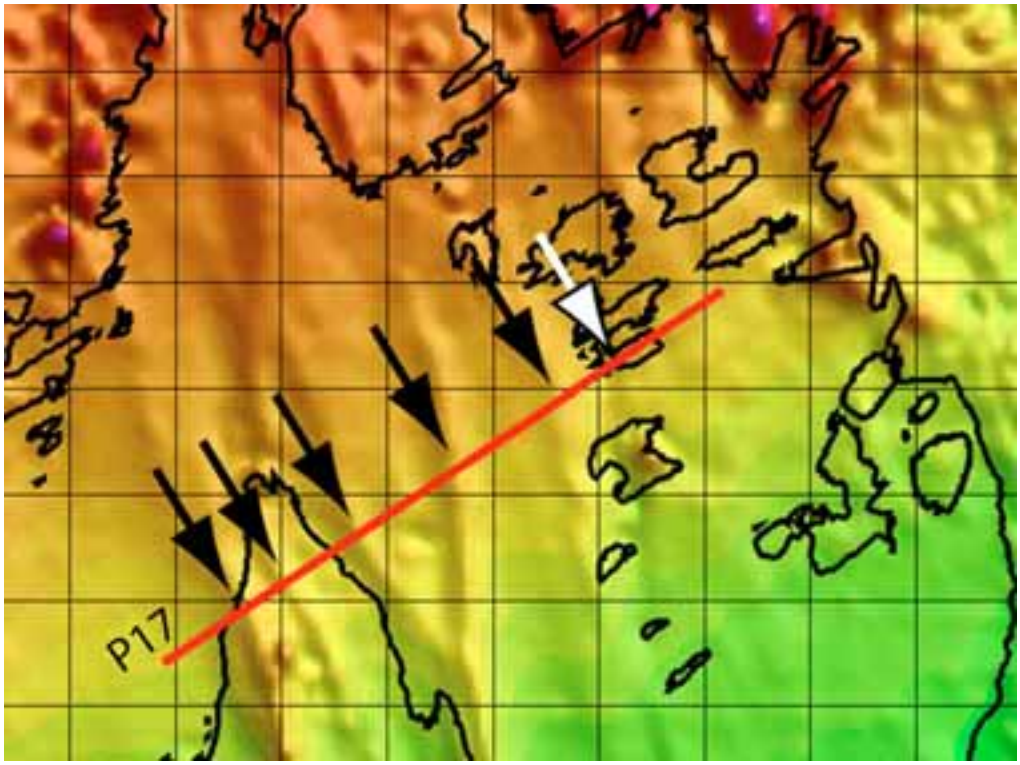

Fig 13 a. Map of inner Oslo Fjord, NE of Nesodden. Black arrows point to positive magnetic anomalies, interpreted as dikes. The white arrow points to a weaker positive anomaly dike that is confirmed to be a dike in the field (Fig. 13b).

Fig. 13b. Photo of N-trending diabase dike on Rambergøya. The dike is marked by a positive anomaly that is partly masked due to being located on the flank of a larger anomaly. Photo Bjørn T. Larsen.

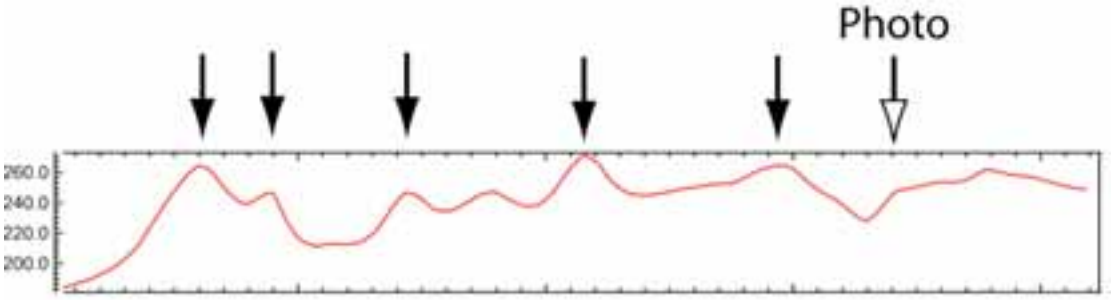

Fig. 13c. Profile 17. Black arrows point to positive magnetic anomalies interpreted to represent N-trending dikes. The white arrow corresponds to an anomaly associated with a proven dike (Fig. 13b).

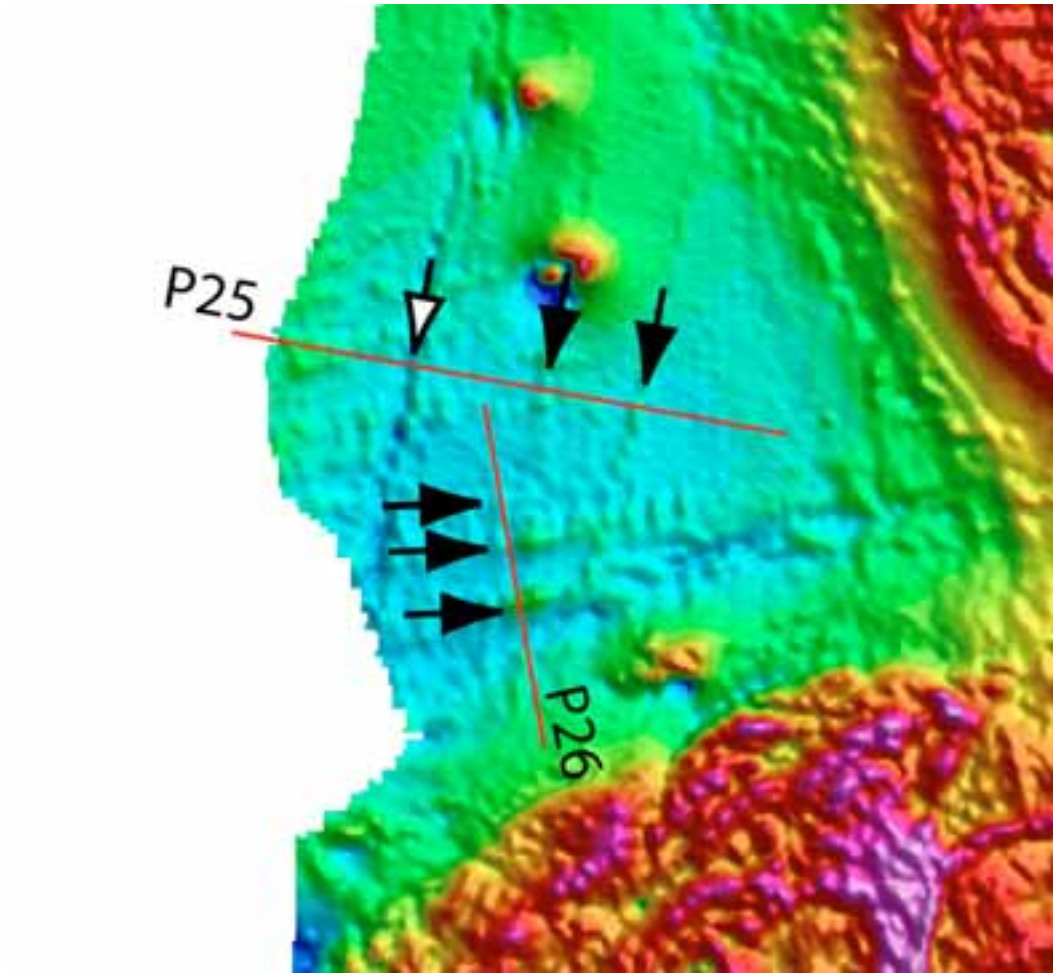

Fig. 14a. Magnetic anomaly map of the Jevnaker area, displaying profiles 25 and 26. Field mapping by J.R. Skilbrei (2004) demonstrated that the negative NNE-trending anomaly marked with a white arrow is mainly a rhomb-porphyry dike. Minor amounts of diabase are present. The black arrows along profile 25 point to positive anomalies that are interpreted to represent diabase dikes. Black arrows along profile 26 point to positive anomalies interpreted to mark faults.

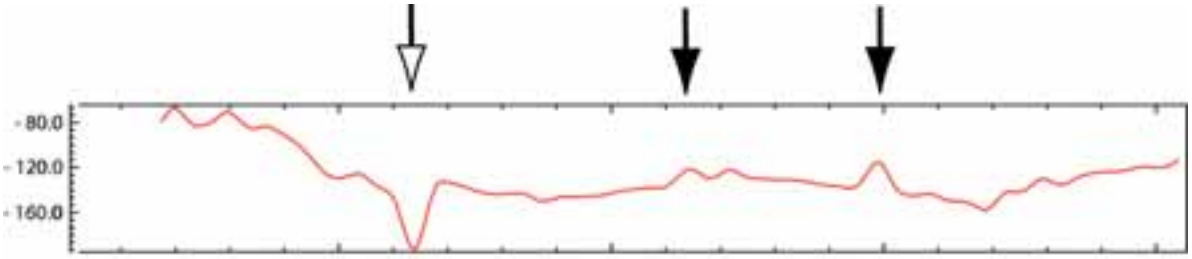

Fig. 14b. Profile 25. The negative anomaly marked by a white arrow is a proven rhomb-porphyry dike. The black arrows point to positive anomalies interpreted as diabase dikes.

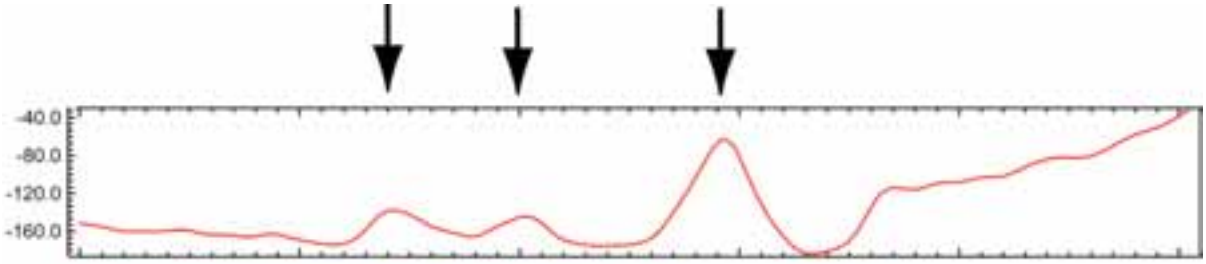

Fig. 14c. Profile 26. The black arrows point to positive anomalies interpreted to represent faults.

2.2 Saprolite – deep tropical weathering.

During drift of the Hvaler tunnel, in the Iddefjord Granite, it was observed that leakage of ground water occurred between the observed "zones of weakness" rather than within them (Banks et al., 1992). Banks et al. (1992) interpreted that the zones of weakness had been hydrothermally altered. More recently, Olesen (2005a and b) concluded that the tightness of these zones relate to clay products stemming from deep weathering during a tropical climate.

Due to the chemical removal of magnetic minerals during the weathering, deeply weathered zones are characterized by negative magnetic anomalies. Such zones are also generally marked by topographic depressions. The realization of this relationship has led to a method for analyzing combined magnetic and topographic data for zones of deep weathering (Olesen, 2005a and b).

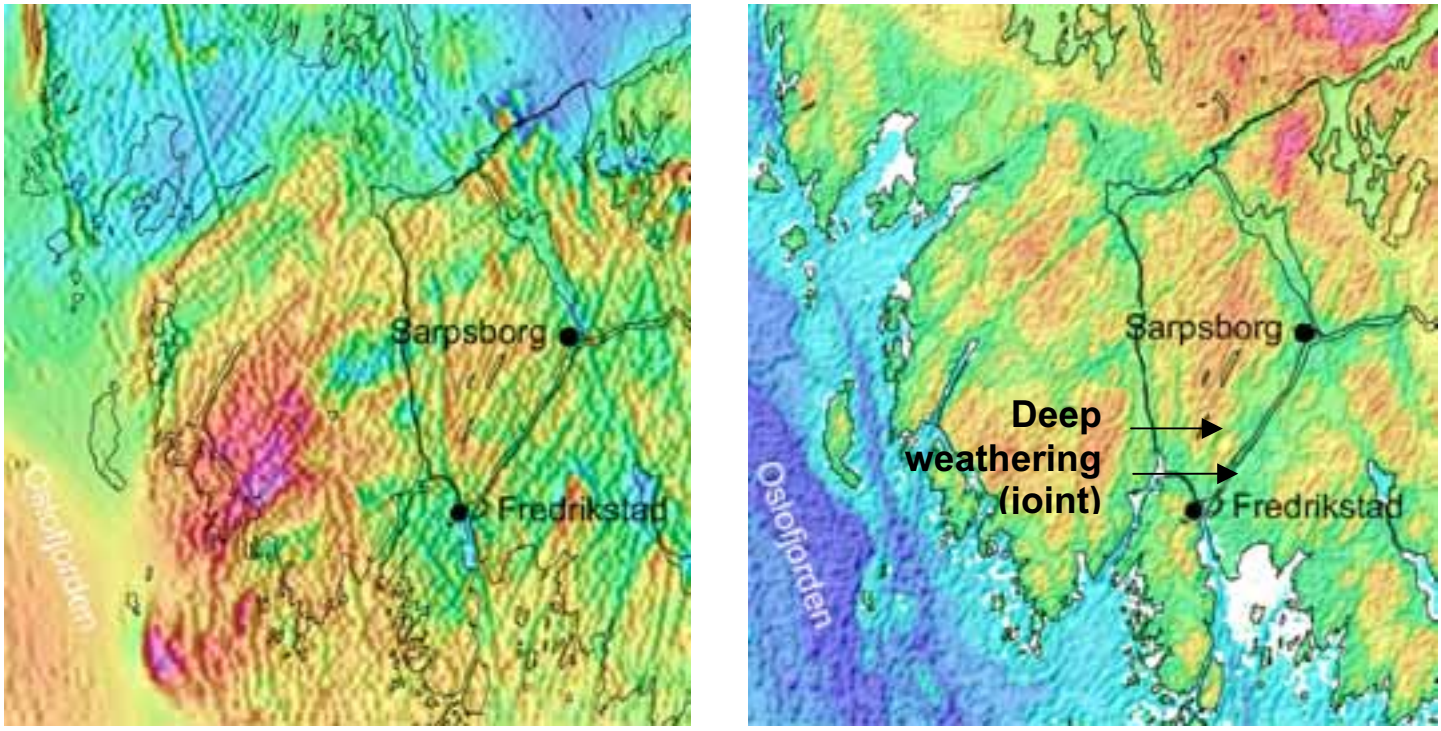

Fig. 15. By combining aeromagnetic data (left) and topographic data (right), areas of deep weathering can be interpreted.


Fig. 16a. Pre-Cretaceous regolith (etch) surface in the Hvaler area.


Fig. 16b. Pre-Cretaceous regolith (etch) surface in the Sarpsborg area. Arrows point to linear topographic depressions.


Fig. 16c. Pre-Cretaceous regolith (etch) surface in the Fredrikstad area. The local linear depressions (Figs. 16a-c), including sounds between islands, are interpreted to represent deeply weathered faults and fracture zones.

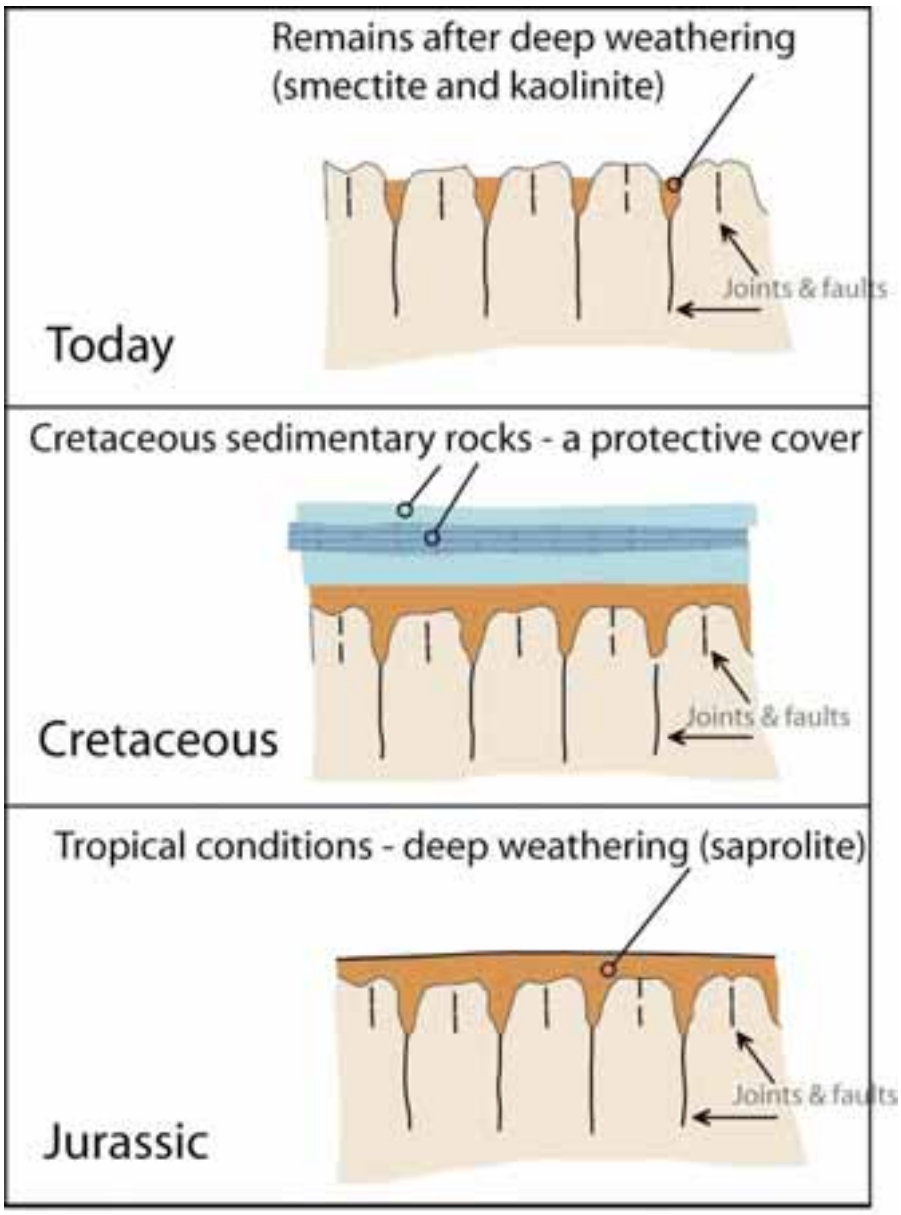

Fig. 17. Schematic illustration of the process leading to the present day deep weathering products. Regolith (etch) surfaces (Figs. 16a-c) in the present day landscape are interpreted to be remnants from Jurassic deep weathering during a tropical climate (modified after Lidmar-Bergström, 1995; Lidmar-Bergström et al., 1999). Clay products (smectite and kaolinite) formed in faults and joints. The clays were probably protected from erosion by a Cretaceous overburden, which is a concept that dates back more than one hundred years, to the pioneering work by Reusch (1902). The overburden was removed in Neogene time during uplift of the Norwegian mainland, leaving an immature etch surface landscape with joints and faults containing smectite and kaolinite. Magnetic minerals were selectively removed from these clays during the weathering, yielding negative magnetic anomalies. Thus, today there is a correspondence between linear topographic depressions and negative magnetic anomalies.

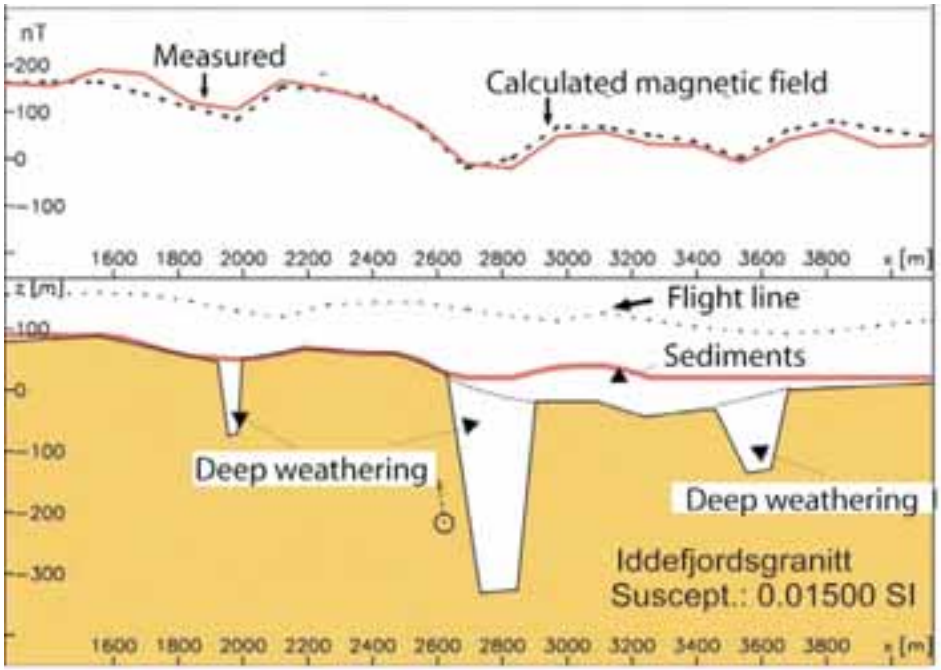

Fig. 18a. Magnetic modelling of a profile (see Fig. 18b for location), supporting that deep weathering is responsible for the linear negative magnetic anomalies associated with linear topographic depressions. The topographic depressions mark weathered faults, fractures, and joints. The white nonmagnetic material represents weathering products (smectite and kaolinite) in which magnetic minerals (magnetite especially) have been oxidized by chemical weathering and leaching (e.g. Grant, 1984).

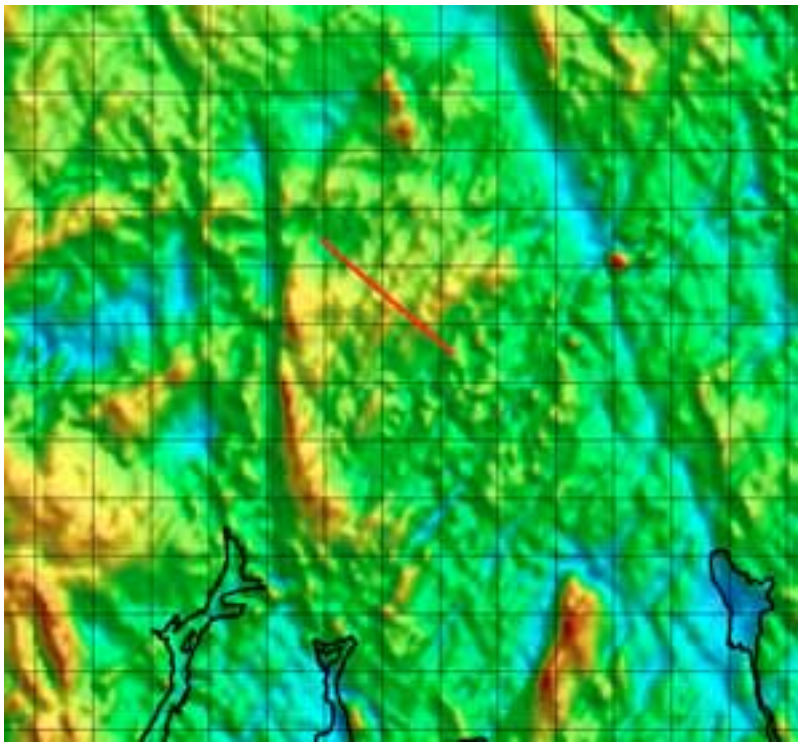

Fig. 18b. Location map for the modelled profile (Fig. 18a)

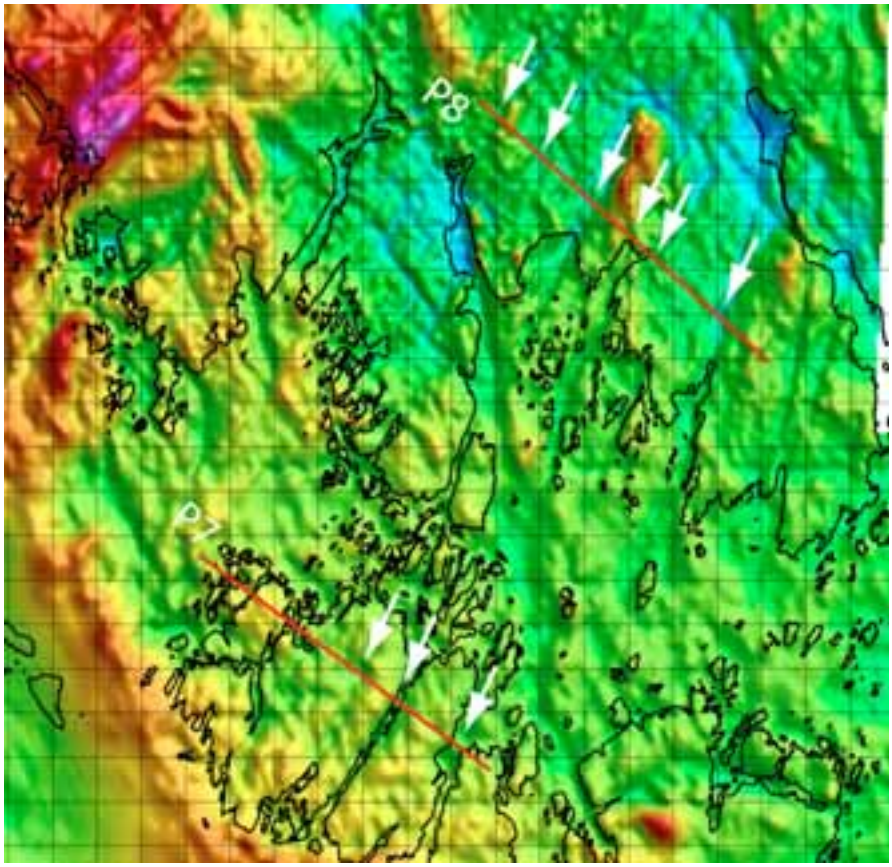

Fig. 19a. Magnetic anomaly map over Fredrikstad area, showing NE-trending negative anomalies interpreted to mark deep weathering. The anomalies typically coincide with topographic depressions.

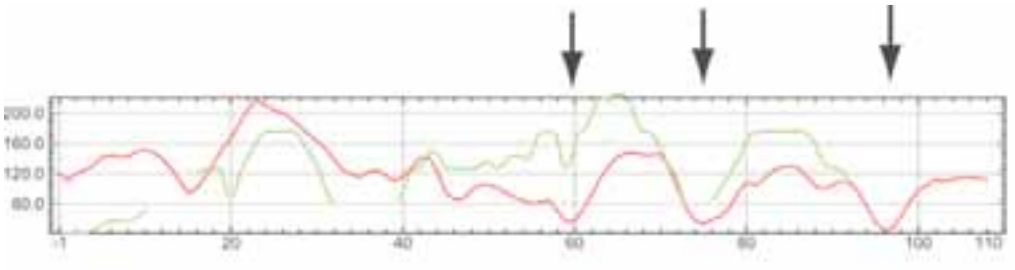

Fig. 19b. Profile 7 over Vesterøy-Spjærøy-Asmaløy (south of Fredrikstad). Marked negative anomalies (red) represent deep weathering. Green curve is topography, illustrating a general correspondence between topographic lows and the negative anomalies.

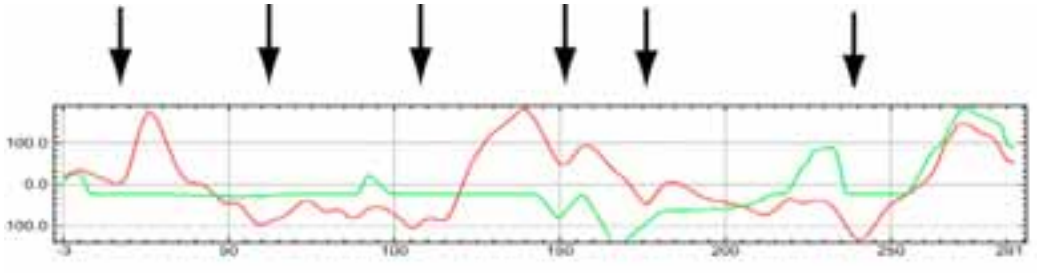

Fig. 19c. Profile 8, located north of Fredrikstad. Marked negative anomalies (red) represent deep weathering. Green curve is topography, illustrating a general correspondence between topographic lows and the negative anomalies.

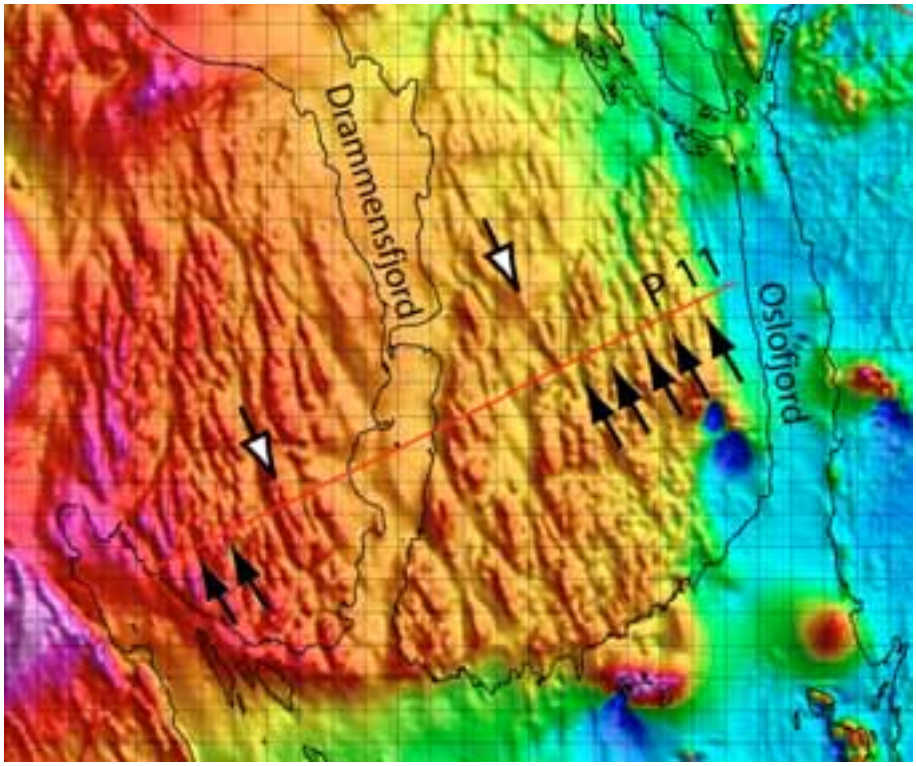

Fig. 20a. Magnetic anomaly map of Hurum area, characterized by NNW-trending anomalies (mainly negative). Negative anomalies are marked with white arrows, while positive anomalies are shown with black and white arrows.

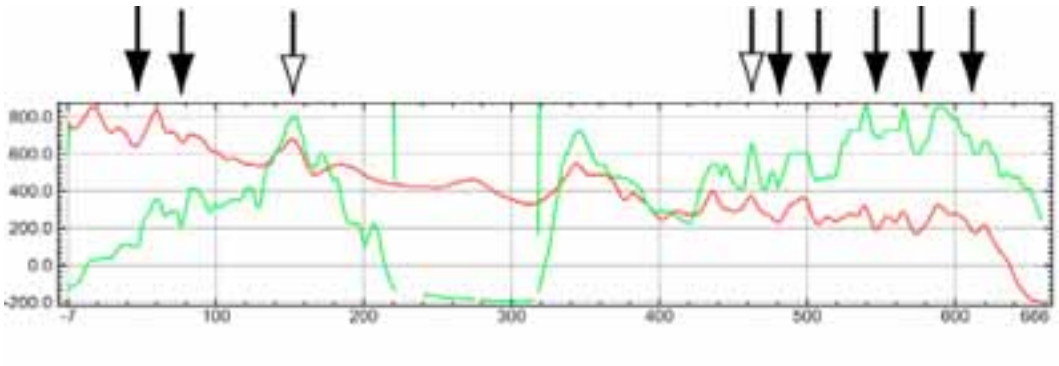

Fig. 20b. Profile 11, revealing a strong relationship between magnetic anomalies and the terrain. The anomalies are interpreted to represent deep weathering. Red curve is magnetic field (associated with the scale on the left side), and green marking topography (no scale included).

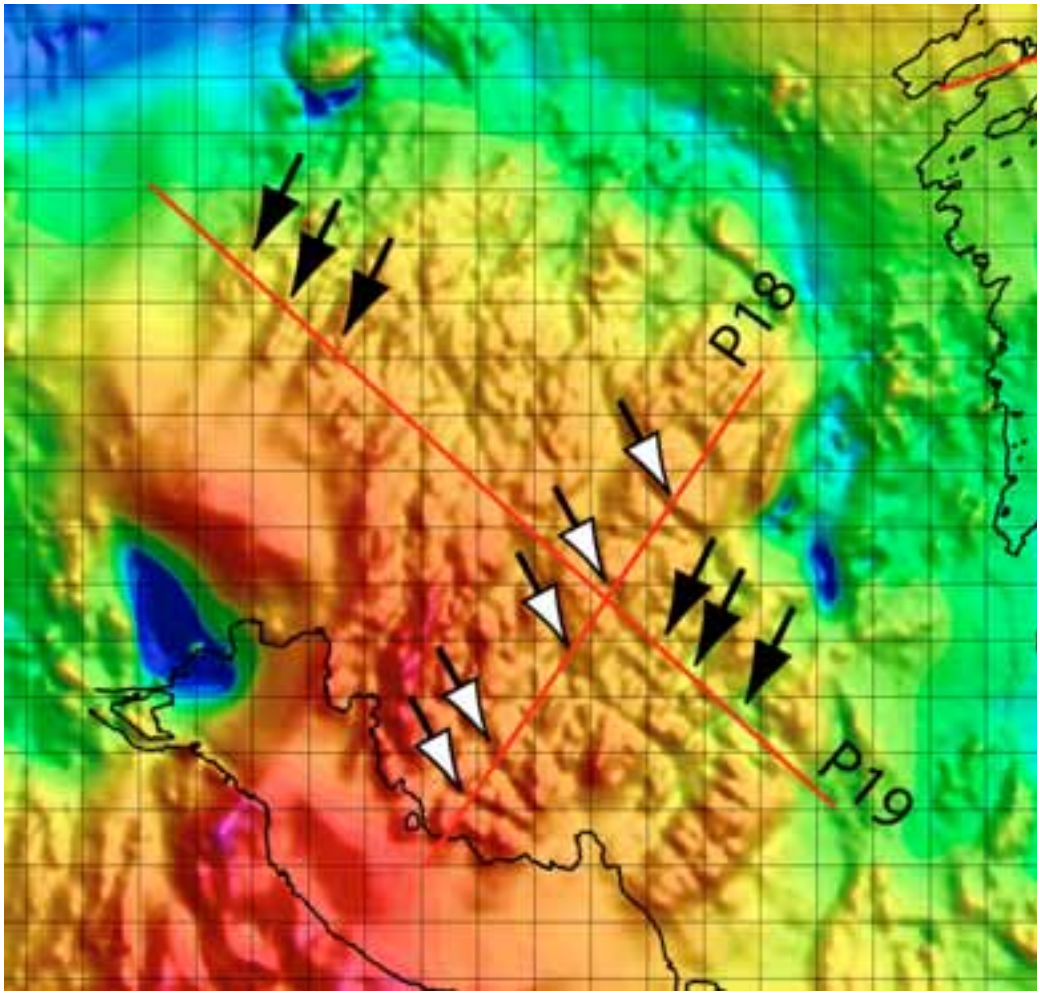

Fig. 21a. Magnetic anomaly map of Drammen area, revealing NW- and NE-trending anomalies.

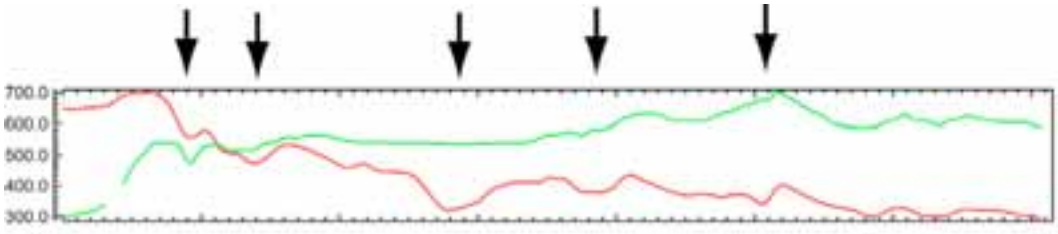

Fig. 21b. Profile 18 showing a general relationship between magnetic anomalies (red) and topography (green). The negative magnetic anomalies are interpreted to relate to deep weathering.

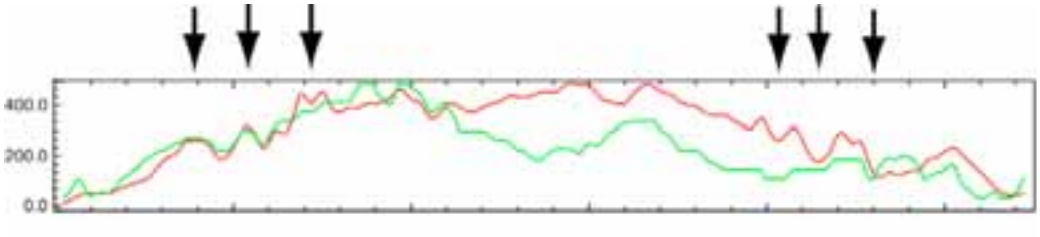

Fig. 21c. Profile 19 also showing a general relationship between magnetic anomalies (red) and topography (green). However, the 3 leftmost black arrows could point to a set of dikes. On a regional scale these anomalies are the northeastern part of a set of NE-trending anomalies that extend between the Sande and Drammen calderas and beyond. The positive anomalies are interpreted as possible dikes. The rightmost 3 anomalies are more likely related to deep weathering.

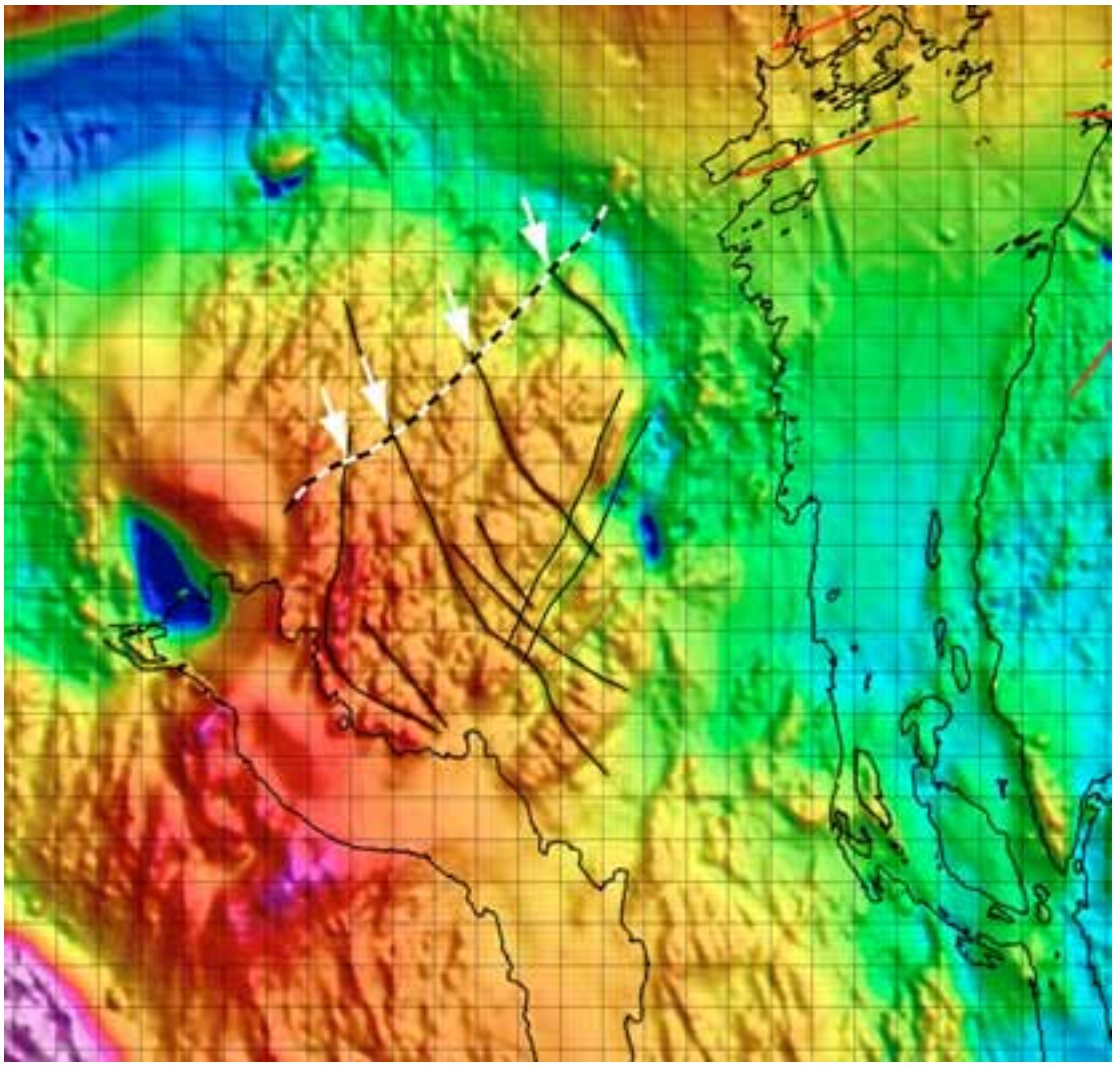

Fig. 22a. Magnetic anomaly map of Lier to Asker area with the Lieråsen railroad tunnel shown in black/white. Black lines are negative magnetic anomalies. White arrows point to the intersection of the negative magnetic anomalies and the tunnel, and are interpreted to represent zones of deep weathering. (compare with Fig 22b).

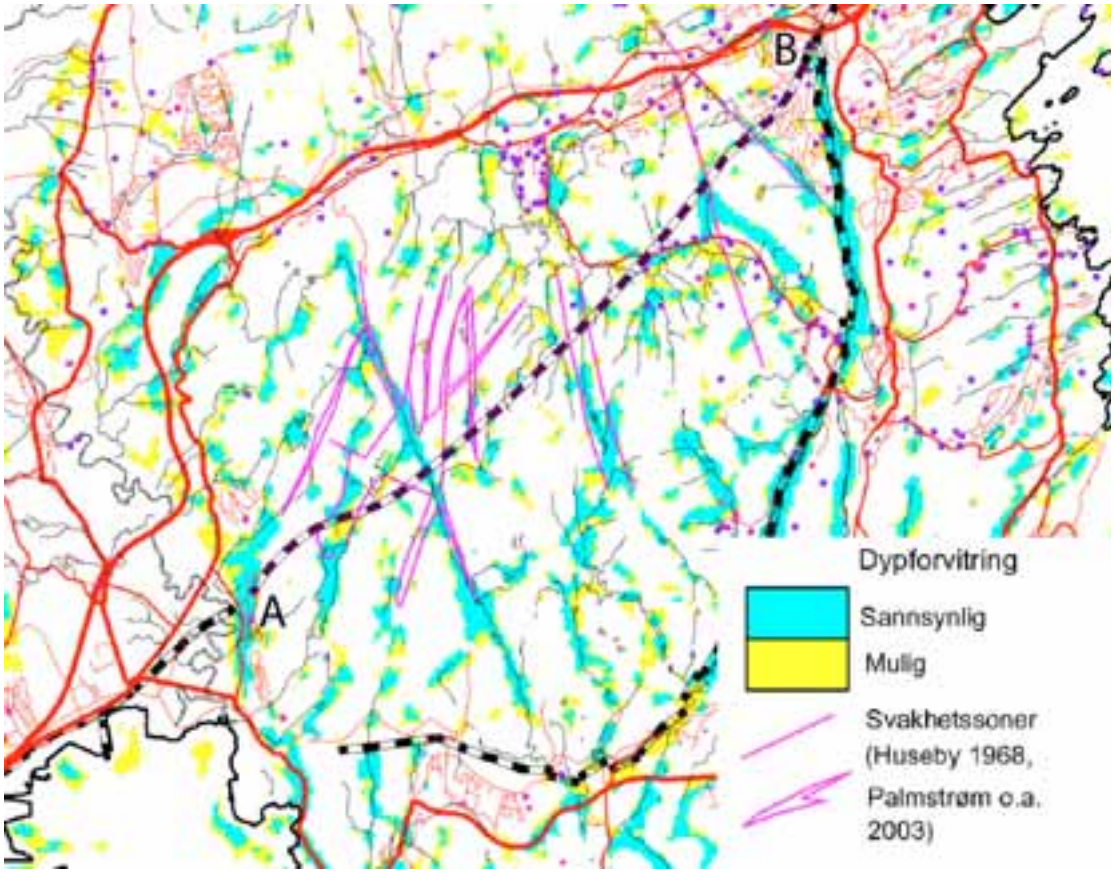

Fig. 22b. Interpreted map of Lier to Asker area with the Lieråsen railroad tunnel (between A and B). Proven weakness zones mapped previously are marked with purple polygons, while predicted zones of deep weathering based on processed magnetic and topographic data are shown in blue (probable) and yellow (possible). O.Olesen, (2005a and b). http://www.ngu.no/FileArchive/217/Info_Dypforvitring.pdf

3. CIRCULAR MAGNETIC ANOMALIES IN THE GEOS AREA

3.1 Anomalies around the Drammen caldera

This section describes a previously not described large elliptical magnetic anomaly located around the Drammen caldera in the Oslo Field. The nature of the c. 22x24 km anomaly is uncertain but could represent the outer limit of the Drammen granitic batholith. Alternatively, it could mark a previously unmapped outer ring fracture zone to the Drammen caldera. The latter possibility seems less likely since there are no mapped indications of a ring fracture zone, nor of any contrasting rock bodies along the anomaly.

.

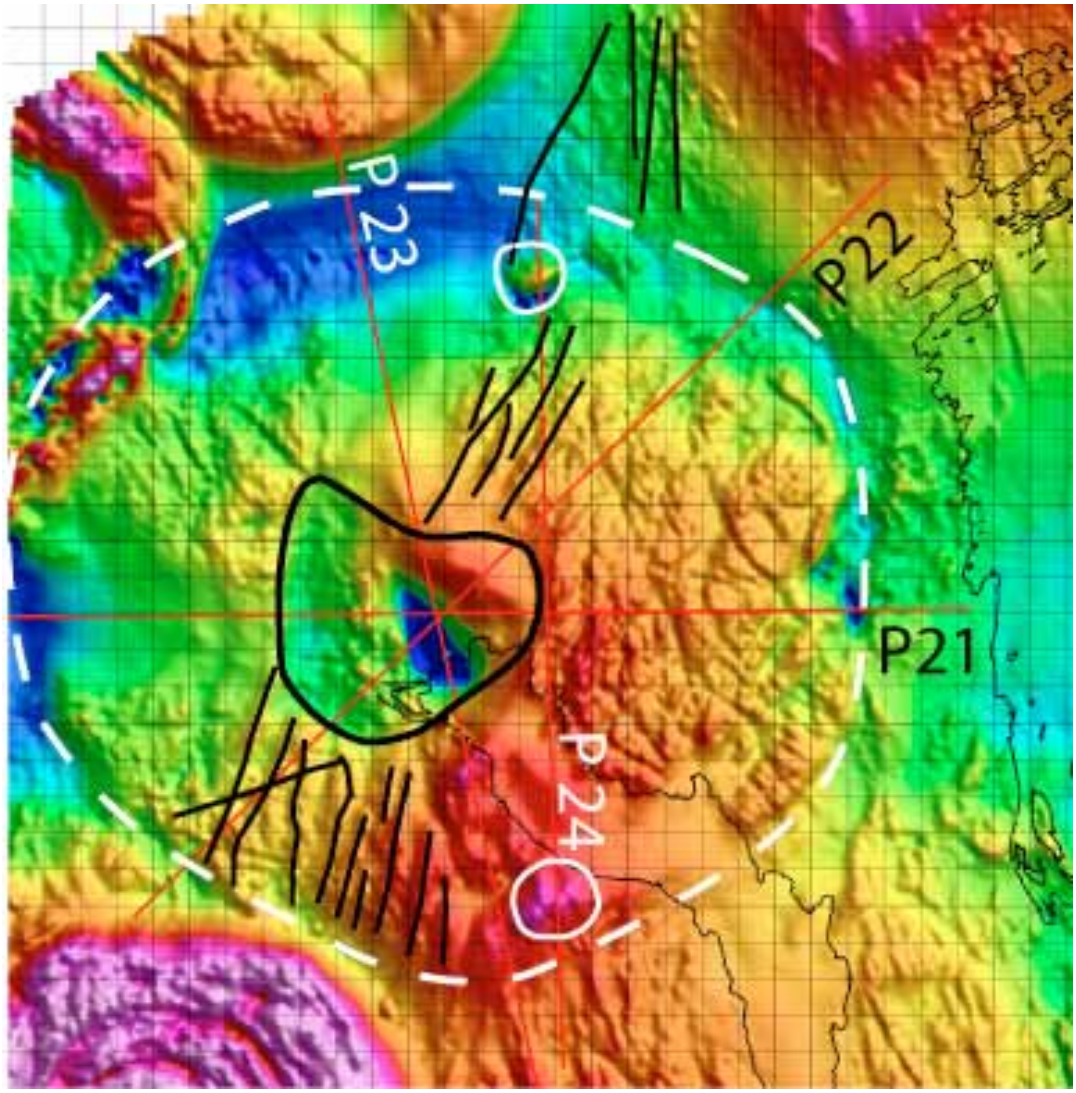

Fig. 23a . Magnetic anomaly map of Drammen caldera area, revealing a previously unreported large circular negative magnetic anomaly (white dashed line). The anomaly is centred about the Drammen caldera (outline in solid black line). In the centre of the Drammen caldera lies a pronounced negative anomaly, of approximately 2000 nT.

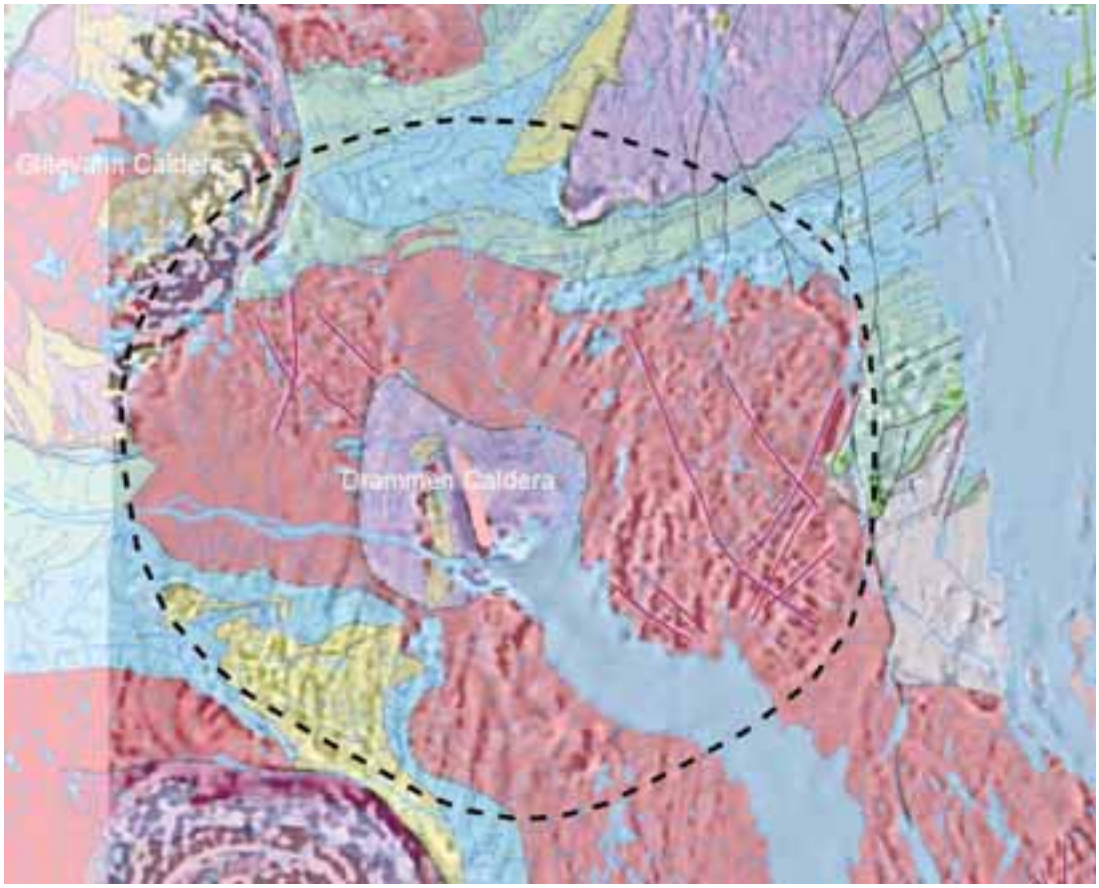

Fig. 23 b. Geologic map of Drammen area draped over the magnetic field. The dashed black line represents the anomaly interpreted in Fig. 22a. The circular anomaly coincides approximately with the northern part of the Drammen granite, and thus the anomaly may mark the batholith.

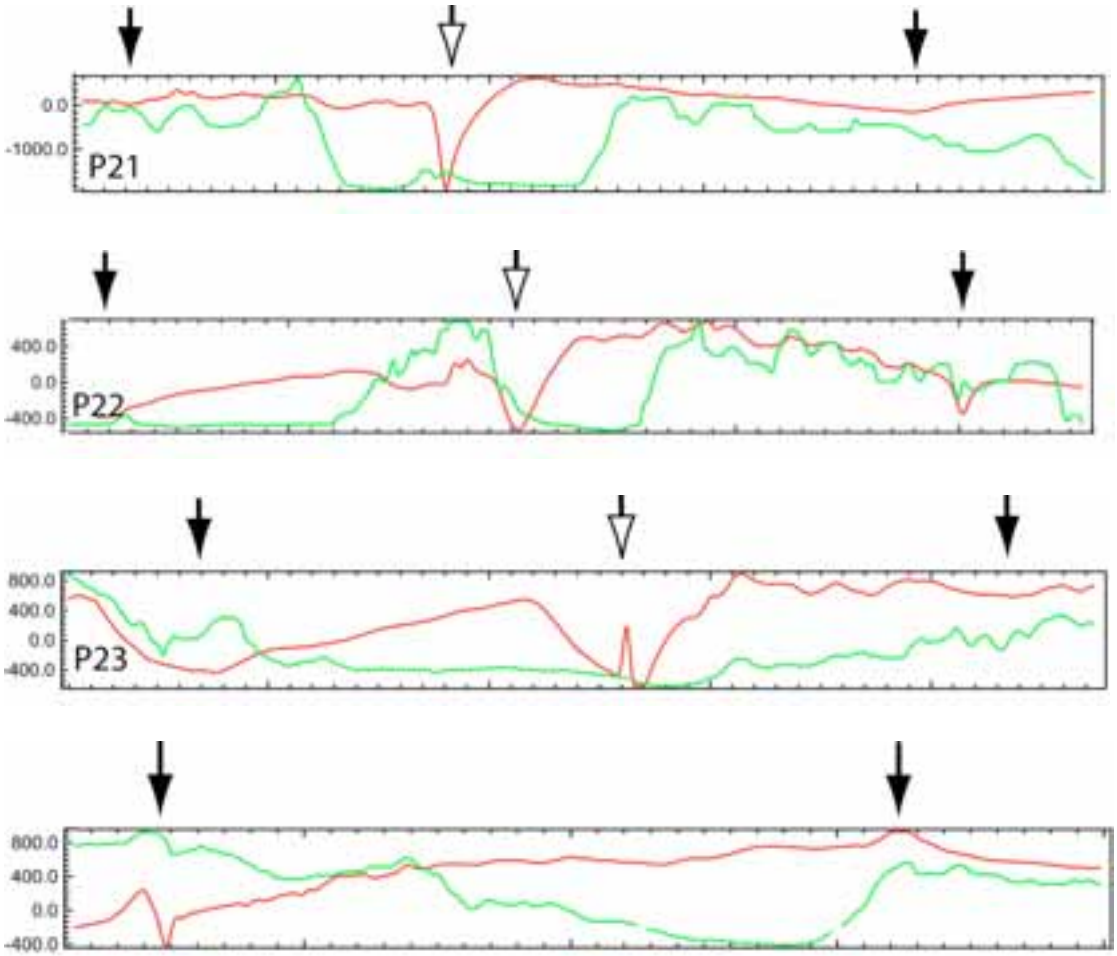

Fig. 23 c. Profiles 21- 24. In. profiles 21-23 the black arrows point to the large circular negative anomaly while the white arrow points to the pronounced negative anomaly On profile 24 the black arrows point to local anomalies located near the large circular anomaly. These local anomalies could relate to smaller late-stage intrusions along the ring fracture zone. See Figs. 23 and 24 for analogs.

Thin NE-trending black lines (see figure 23a) mark positive anomalies, and may represent a dike swarm along trend between the Sande caldera to the SW and the Drammen caldera. The nature of the pronounced central negative anomaly is uncertain but could relate to basalts. Alternatively, the anomaly could represent a late stage central intrusion. If so, the intrusion is not exposed, or at least not recognized, at the surface. The nature of the two negative and positive anomalies outlined with white circles is also unknown but could represent late-stage intrusions along an outer ring fracture zone, by analogy with other calderas. For comparison see Figs. 24-26.

3.2 Caldera model and analogs

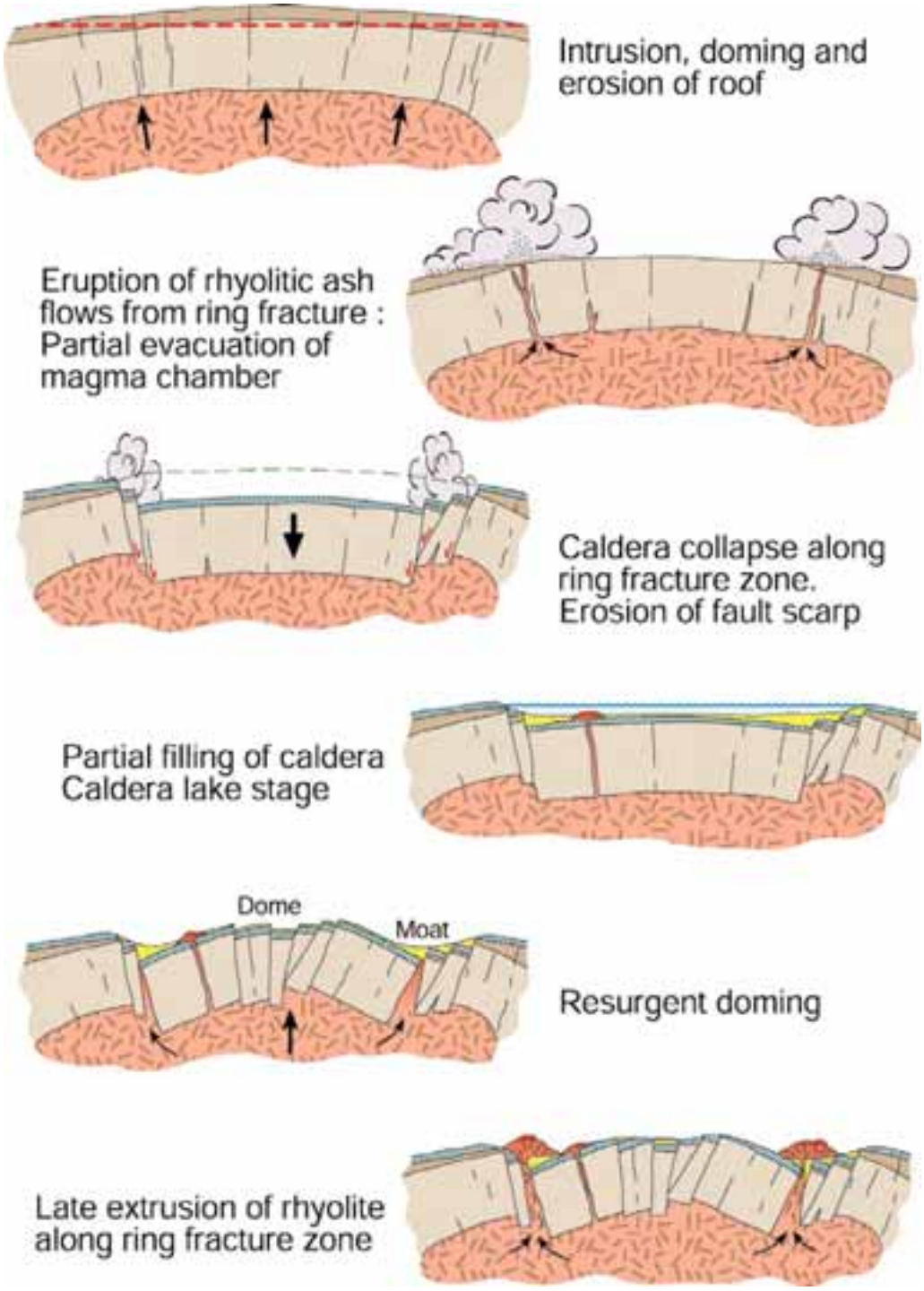

Fig. 24. Generalized evolution of an ashflow caldera. The large circular anomaly around the Drammen caldera could relate to the outline of a batholith, inside which the Drammen caldera is located. Alternatively, the large circular anomaly could relate to an outer ring fracture zone that is either poorly known from mapping, or only faintly expressed by lithologic changes. The innermost pronounced negative anomaly could either relate to basalts located centrally in the Drammen caldera, or alternatively could relate to a central late stage intrusion formed during resurgence. From Smith and Bailey, 1968.

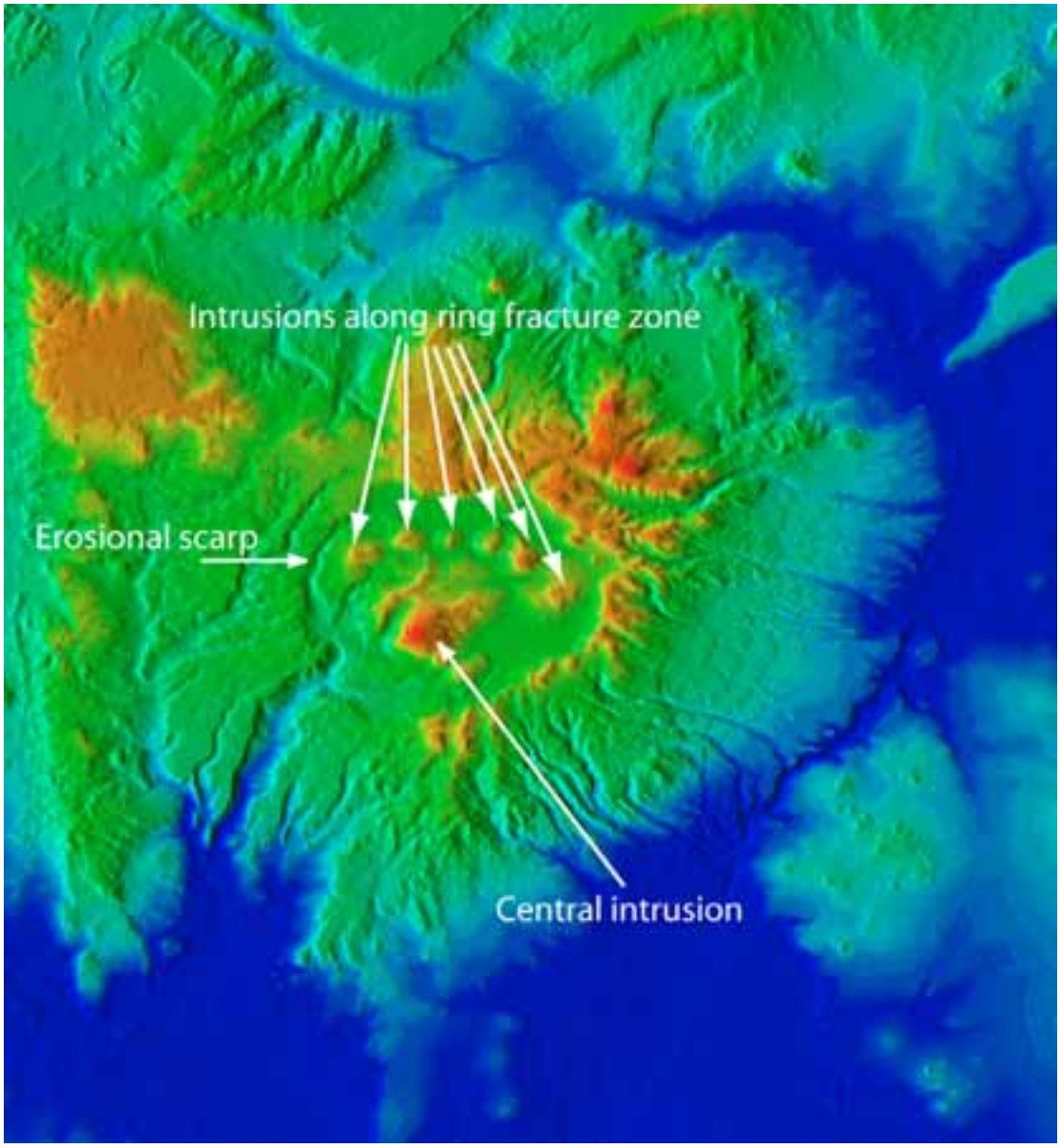

Fig. 25. Shaded topographic image of the Valles caldera, New Mexico. Geomorphologically, this Pleistocene age caldera (c. 1.1 Ma) is very prestine. The image clearly reveals the erosional caldera scarp, a series of intrusions located above the ring fracture zone, and a late-stage high located centrally in the caldera. The long axis of the ellipse describing the erosional scarp measures approximately 22 km. The Valles caldera served as the main source for the conceptual caldera evolution illustrated in Fig 24.

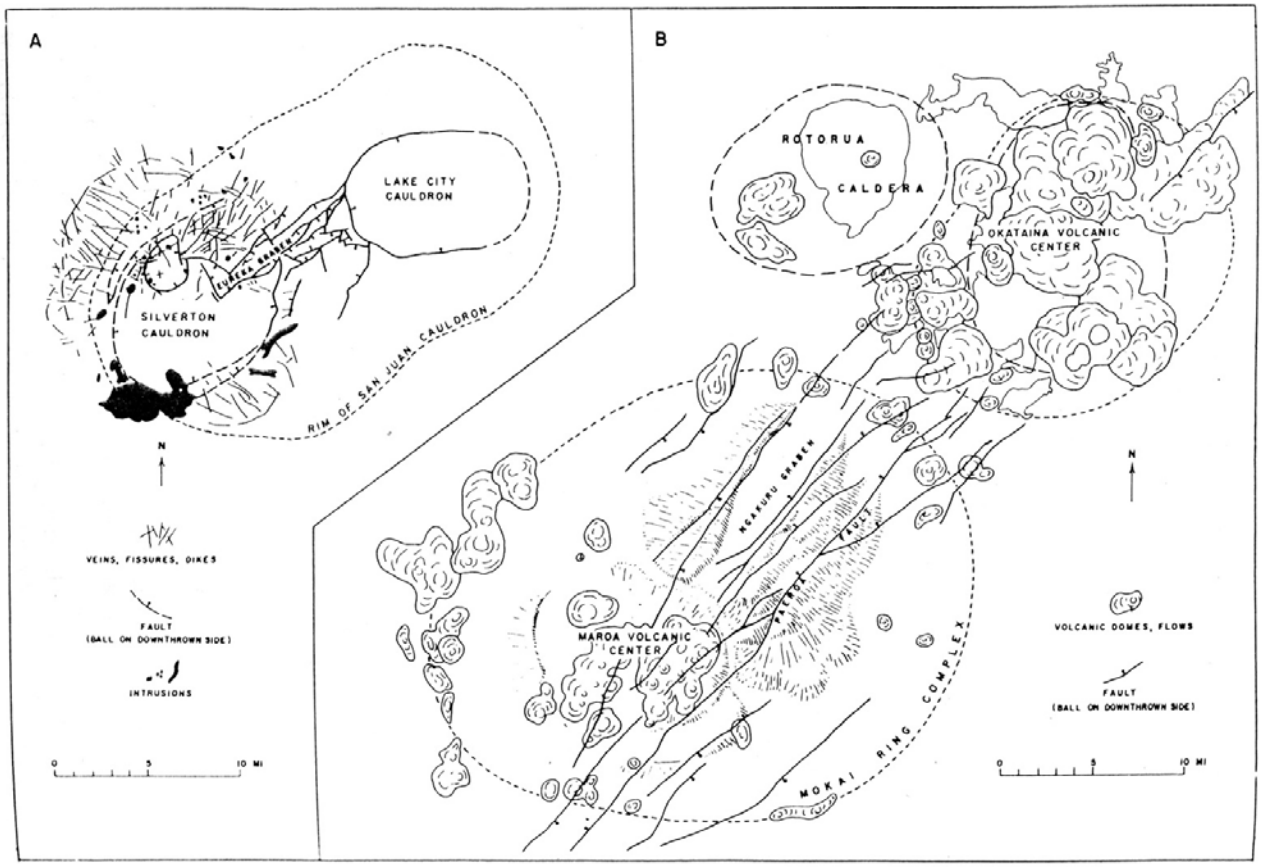

Fig. 26. Structure maps of a) the Silverton/Lake City calderas in the San Juan Mountains, Colorado, and b) the Maroa/Okataina/Rotorua calderas in north Iceland. Note the fault system between the calderas and compare with Fig. 23a. From Smith and Bailey, 1968.

4. CONCLUSIONS

- Magnetic anomalies in the Oslo region can be grouped into two general groups:
  1) Those associated with the Precambrian basement and the Paleozoic cover rocks.
  2) Those associated with the Permian magmatic rocks.

- Permian magmatic rocks can be subdivided into:
  a) linear anomalies.
  b) circular to elliptical anomalies related to calderas and plutons, and

- The linear anomalies have several origins and do not only stem from Permian age rocks. The anomalies can be related to:
  a) faults of various age and origin (with or without Permian dike intrusions)
  b) Permian dikes
  c) joints and fractures deeply weathered in Mesozoic time (mainly Jurassic time).

- Dikes are for the most part positive anomalies, although examples of negative anomalies exist. Especially the large rhomb-porphyry dikes tend to be characterized by negative anomalies. Most diabase dikes are characterized by positive anomalies.

- Dikes are generally groundwater bearing due to them being highly fractured.

- Deeply weathered joints and fractures are characterized by negative anomalies due to the oxidation of iron-bearing minerals. These anomalies tend to coincide with linear topographic depressions.

- Deeply weathered joints and fractures, were weathered during a tropical climate and thus contain smectite and kaolinite. Such tight clays prohibit groundwater flow. However, such clay-filled zones can cause mechanical problems during tunnel drift. Water break-through in tunnels driven across deeply weathered joints and fractures tend to occur between the structures.

5. REFERENCES CITED

Acworth, R.I. 1987: The development of crystalline basement aquifers in a tropical environment. Quarterly Journal of Engineering Geology, v. 20, p. 265-272.

Banks, D., Rohr-Torp, E. & Skarphagen, H., 1992: An integrated study of a Precambrian granite aquifer, Hvaler, Southeastern Norway. NGU Bulletin, 422, p. 47-66.

Beard, L.P. 1998: Data acquisition and processing - helicopter geophysical survey, Oppkuven and Gran, 1997. NGU-report 98.079, 20 pp.

Beard, L.P. 1999: Data acquistion and processing - helicopter geophysical surveys, Larvik, 1998. NGU-report 99.026, 13 pp.

Beard, L.P. og Mogaard, J.O. 2001: Data acquisition and processing - helicopter geophysical survey, Hurdal, 2000. NGU-report 2001.018, 16 pp.

Beard, L.P. og Rønning, S. 1997: Data aquisition and processing report - helicopter geophysical survey, Krokskogen. NGU-report 97.134, 9 pp.

Fugro Airborne Surveys Central Region 2003: Logistics report, fixed wing borne magnetic, radiometric and VLF-EM survey in the Oslo region, southern Norway. Report FCR 2241, 124 pp.

Grant, F.S., 1984, Aeromagnetics, geology and ore environments, I. Magnetite in igneous, sedimentary and metamorphic rocks: an overview. Geoexploration, v. 23, p. 303-333.

Håbrekke, H. 1982: Magnetiske-, elektromagnetiske-, VLF- og radiometriske målinger fra helikopter over et område vest for Tønsberg, Vestfold og Telemark fylker. NGU-report 1835, 13 pp.

Lidmar-Bergström, K. 1995: Relief and saprolites through time on the Baltic Shield. Geomorphology, v. 12, p. 45-61.

Lidmar-Bergström, K., Olsson, S., & Roaldset, E., 1999: Relief features and palaeoweathering remnants from formerly glaciated Scandinavian basement areas. In: Thirty, M. & Simon-Coincon, R. (eds). Palaeoweathering, Palaeosurfaces, and Related Continental Deposits, Spec. Publ. 27, International Association of Sedimentologists, p. 275-301, Blackwell.

Mogaard, J.O. 1998: Geofysiske målinger fra helikopter ved Larvik, Vestfold. NGU-report 98.021, 11 pp.

Mogaard, J.O. 2001: Geofysiske målinger fra helikopter ved Sandefjord, Vestfold 2000. NGU-report 2001.003, 12 pp.

Mogaard, J.O. og Beard, L.P. 2000: Geofysiske målinger fra helikopter ved Skien, Telemark 1999. NGU-report 2000.031, 12 pp.

Olesen, O**.** 2005a: Problemene skyldes dypforvitring. *GEO 7, 18-20*.

Olesen, O. 2005b: Ny metode for kartlegging av dypforvitring. *GEO 7, 20***.**

Reusch, H., 1902: Vore dale og fjelde. Hvordan formen af Norges overflade er dannet. Naturen, v. 26, p. 29-142.

Smith, R.L. and Bailey, R.A. 1968: Resurgent cauldrons, Gelogical Society of America Mamoir 116, p. 613-662.

Map 7 - Interpreted magnetic anomalies in the Oslo area overlain on Oslo Field geologic map.